

**UNIVERSIDADE FEDERAL DO ESPÍRITO SANTO
CENTRO TECNOLÓGICO
DEPARTAMENTO DE ENGENHARIA MECÂNICA**

BRENO VENTORIM DE TASSIS

**AVALIAÇÃO E OTIMIZAÇÃO DA PERFORMANCE AERODINÂMICA
DO VEÍCULO TARF-LCV**

**VITÓRIA
2016**

BRENO VENTORIM DE TASSIS

**AVALIAÇÃO E OTIMIZAÇÃO DA PERFORMANCE AERODINÂMICA
DO VEÍCULO TARF-LCV**

Projeto de Graduação apresentado ao
Departamento de Engenharia Mecânica da
Universidade Federal do Espírito Santo,
como requisito parcial para obtenção do
título de Engenheiro Mecânico.

Orientador: Prof. Dr. Bruno Venturini Loureiro

VITÓRIA

2016

BRENO VENTORIM DE TASSIS

**AVALIAÇÃO E OTIMIZAÇÃO DA PERFORMANCE AERODINÂMICA
DO VEÍCULO TARF-LCV**

Trabalho de conclusão de curso apresentado ao Departamento de Engenharia Mecânica da Universidade Federal do Espírito Santo, como requisito parcial para obtenção do título de Engenheiro Mecânico.

COMISSÃO EXAMINADORA

Prof. Dr. Bruno Venturini Loureiro
Universidade Federal do Espírito Santo
Orientador

Prof. Oswaldo Paiva Almeida Filho
Universidade Federal do Espírito Santo
Examinador

Bruno Filipe da Penha Sperandio, mestrando.
Universidade Federal do Espírito Santo
Examinador

ACKNOWLEDGMENTS

First, I would like to take this opportunity to thank Mr Amit Prem, my project supervisor at Coventry University. Without his contribution, monitoring and guidance this report would not have been written.

Special thanks and my gratitude should be given to Mr Bill Dunn, who supported me during this great year at Coventry University. His support, help, advices and constant encouragement throughout the academic year were of paramount importance.

I would also like to thanks the former student Dalvy, who helped me setting the first CFD simulation for the TARF-LCV model.

Last, but not least, I would like to mention my supervisor at Universidade Federal do Espírito Santo, Bruno Venturini Loureiro.

ABSTRACT

Towards Affordable, Closed-Loop Recyclable Future Low Carbon Vehicle or, simply, TARF-LCV. It is a £5 million project led by Brunel University in partnership with 7 other British universities and funded by Engineering and Physical Sciences Research Council (EPSRC).

The TARF-LCV project was created due to big challenges that United Kingdom's automotive industry is facing in the last years, such as been responsible for a 19% growing share of UK annual CO₂ emissions. TARF-LCV aims to deliver fundamental solutions to the key challenges faced by future development of Low Carbon Vehicles (LCV) (Research Councils UK, 2013).

This project is **mainly focused** on analysing and evaluating the aerodynamics of the **6th TARF-LCV concept** developed in Coventry University, one of the 8 UK universities members of TARF-LCV research team.

To do so, a brief literature review of vehicle aerodynamics and a case study of previous TARF-LCV concepts was written.

Keywords: 1. Aerodynamics; 2. Drag; 3. Lift; 4. Vehicle; 5. Optimisation.

SUMMARY

LIST OF FIGURES	8
LIST OF TABLES	9
LIST OF GRAPHS	9
GLOSSARY	10
1. INTRODUCTION	11
2. PROJECT OBJECTIVES	12
3. LITERATURE REVIEW	12
3.1. PRINCIPLE AND FUNDAMENTALS OF AERODYNAMICS	12
3.1.1. STREAMLINES	12
3.1.2. BOUNDARY LAYERS	12
3.1.3. LAMINAR AND TURBULENT FLOWS	13
3.1.4. FLOW SEPARATION	14
3.1.5. REYNOLDS NUMBER	14
3.1.6. DRAG AND LIFT FORCES	14
3.1.7. DRAG AND LIFT COEFFICIENTS	15
3.2. HOW TO IMPROVE AERODYNAMIC PERFORMANCE	16
3.2.1. WIND TUNNEL TESTING	16
3.2.2. DESIGN DEVELOPMENT	16
3.2.3. DEVICES AND GENERAL IMPROVEMENTS	19
4. TARF-LCV PREVIOUS CONCEPTS CASE STUDY	20
4.1. CONCEPT #1	20
4.1.1. CHARACTERISTICS.....	20
4.1.2. AERODYNAMIC ANALYSIS	21
4.2. CONCEPT #2	23
4.2.1. MODIFICATIONS	23
4.3. CONCEPT #3	25
4.3.1. MODIFICATIONS	25
4.3.2. AERODYNAMIC ANALYSIS	26
4.4. CONCEPT #4	28
4.4.1. MODIFICATIONS	28
4.4.2. AERODYNAMIC ANALYSIS	28
4.5. CONCEPT #5	30
5. METHODOLOGY – MODELLING THE CONCEPT #6 CFD SIMULATION	31

6. CONCEPT #6 – CFD RESULTS	36
7. CONCLUSION.....	42
8. REFERENCES	45
APPENDIX A – Volume Meshes	46
APPENDIX B – Residuals Plot.....	48

LIST OF FIGURES

Figure 1- Streamlines (Barnard, 2009)	12
Figure 2- Boundary Layers (Barnard, 2009).....	13
Figure 3- Flow around a Passengers Car (Ahmed et al, 1998)	13
Figure 4- Aerodynamic Forces (Accessed in http://www.kasravi.com/cmu/tec452/aerodynamics/VehicleAero.htm)	14
Figure 5- Drag Forces (Accessed in http://www.up22.com/Aerodynamics.htm).....	15
Figure 6- Lift Forces (Accessed in http://www.up22.com/Aerodynamics.htm).....	15
Figure 7- Different front end shapes and drag coefficient (Vasiu et al, 2013).....	16
Figure 8- Conical Vortices Generated on Hatchback (Vasiu et al, 2013)	17
Figure 9- Effective Rear Slope Angle (Vasiu et al, 2013)	18
Figure 10- General Improvements (Accessed in http://www.kasravi.com/cmu/tec452/aerodynamics/VehicleAero.htm)	19
Figure 11- TARF-LCV 1st concept	20
Figure 12- Concept #1 Streamlines.....	21
Figure 13- Concept #1 Pressure Coefficient.....	22
Figure 14- Concept #1 Velocity Field	23
Figure 15- Concepts #1 and #2 Front-end	24
Figure 16- Concepts #1 and #2 Side body	24
Figure 17- Concepts #1 and #2 Rear-end	24
Figure 18- Concept #3 Mesh Scene	25
Figure 19- Concepts #2 and #3 Front-end	26
Figure 20- Concepts #2 and #3 Side body	26
Figure 21- Concepts #2 and #3 Rear-end	26
Figure 22- Concept #4 Velocity Field	27
Figure 23- Concept #4 Pressure Coefficient.....	27
Figure 24- Concept #4 Final Design.....	28
Figure 25- Concept #4 Pressure Coefficient.....	29
Figure 26- Concept #4 Velocity Field	29
Figure 27- Concept #4 Streamlines.....	29
Figure 28- Vortex Core and Flow Separation	30
Figure 29- Surface Wrapper Properties.....	32
Figure 30- Surface Diagnostic	33
Figure 31- Wind Tunnel.....	33
Figure 32- Frontal Area Report.....	36
Figure 33- Drag Coefficient Report.....	37
Figure 34- Lift Coefficient Report.....	37
Figure 35- Distance Vehicle - Floor	37
Figure 36- Velocity Distribution Vectors	39
Figure 37- Velocity Magnitude around Vehicle	39
Figure 38- Wake formation (front view)	40
Figure 39- Wake formation (rear view)	40
Figure 40- Pressure Coefficient Distribution (Front view)	41
Figure 41- Pressure Coefficient Distribution (Rear view).....	41
Figure 42- Recommended Modifications	43

Figure 43- Recommended Modifications	44
--	----

LIST OF TABLES

Table 1- Concept #1 CFD Results.....	22
Table 2- Concept #3 CFD Results.....	26
Table 3- Concept #4 CFD Results.....	28
Table 4- Concept #5 CFD Results.....	30
Table 5- Wind Tunnel Regions Properties.....	33
Table 6- Mesh Continuum Reference Values.....	34
Table 7- Base Sizes and CFD Results	36
Table 8- Concept #6 CFD Results.....	36

LIST OF GRAPHS

Graph 1- Windshield Angle influences on Drag Coefficient (Ahmed et al, 1998).....	17
Graph 2- Underbody Diffuser (Barnard, 2009)	18
Graph 3- Roof Shape influences on Drag Coefficient (Ahmed et al, 1998)	19
Graph 4- Concept #5 Drag Force Distribution	31
Graph 5- Concept #5 Lift Force Distribution	31
Graph 6- Accumulated Drag Force.....	38
Graph 7- Accumulated Lift Force.....	38
Graph 8 - Drag and Lift Coefficients Evolution	42
Graph 9 - Cd vs Mesh base size	43

GLOSSARY

Abbreviations

2D	Two Dimensional
3D	Three Dimensional
A	Frontal Area of a car [m ²]
C_D	Drag Coefficient
C_L	Lift Coefficient
CAD	Computer Aided Design
CATIA	Computer Aided Three-dimensional Interactive Application Software
CFD	Computational Fluid Dynamics
CO ₂	Carbon Dioxide
D	Drag Force [N]
ELV	End of Life Vehicle
EPSRC	Engineering and Physical Sciences Research Council
L	Lift Force [N]
l	Length of a body [m]
LCV	Low Carbon Vehicle
OPEC	Organization of the Petroleum Exporting Countries
R	Radius [in]
Re	Reynolds Number
STAR-CCM+	Computer Aided Design Software used for CFD analysis
TARF-LCV	Towards Affordable, Closed Loop Recyclable Future Low Carbon Vehicle
V, v	Velocity [m/s]
μ	Fluid Viscosity
ρ	Air Density [kg/m ³]

Units

in	Inches
kg	Kilogram
m	Meter
m ²	Meter squared
m ³	Cubic meter
min	Minute
mm	Millimetres
s	Second

1. INTRODUCTION

During the first years of the automotive industry, vehicle aerodynamics was only taken in consideration when designing racing cars.

The major impetus to serious attempts at drag reduction for mass-produced vehicles came in 1973 when a group of oil exporting countries (OPEC) formed a cartel, drastically increasing the price of crude oil, and simultaneously cutting production (Barnard, 2009).

The shortage of fuel in the market at that time frightened the automotive industry. Automakers had to invest in the production of cars with lower fuel consumption.

The fuel consumption of a vehicle depends on the efficiency of the engine and transmission system, and the power required to overcome the resistance to motion. The required power is the product of the total resistance force, and the vehicle speed.

$$\text{Power} = \text{total resistance force} \times \text{speed}$$

At steady speed on a level road, the total resistance to motion is the sum of two separate contributions, aerodynamic drag, and tyre rolling resistance (Barnard, 2009).

From the last two decades, emissions standards for road vehicles have been created by governments and commissions around the world, setting specific limits to the amount of gas emissions that vehicles can release to the atmosphere. For instance, UK Department for Transport (DfT) set a challenging aim of 60% reduction in CO₂ emission from road vehicles by 2030.

A solution to these challenges comes from the development and manufacture of low carbon vehicles, as identified by the UK government. Vehicle lightweighting is the most effective way to improve fuel economy and to reduce CO₂ emissions. This has been demonstrated by many vehicle mass reduction programmes worldwide (Research Councils UK, 2013).

In fact, a 10% reduction in drag can result in approximately 4% reduction in fuel consumption combined. This is valid only if the reduction of air drag is achieved by re-matching of the gear ratios. Reduction in drag by 20-50% results in reduction of fuel consumption of 8-20% respectively (Businaro et al, 1983).

Therefore, low drag is important for good fuel economy and low emissions. But the other aspects of vehicle aerodynamics are no less important for the quality of an automobile: directional stability; wind noise; soiling of the lights, windows and body; cooling of the engine, gearbox and brakes; and finally, heating ventilating and air conditioning of the passenger compartment. (Ahmed et al, 1998).

2. PROJECT OBJECTIVES

- ❖ To analyse and evaluate aerodynamic performance of TARF-LCV concept #6 architecture;
- ❖ To find critical points on the vehicle structure that may cause an increase in aerodynamic drag force and coefficient;
- ❖ To modify the design of some parts of the vehicle, such as bumpers and rear diffusers in order to improve aerodynamic performance, reducing vehicle drag;
- ❖ To perform different CFD simulations to check if modifications achieved the expected overall results;
- ❖ To suggest external modifications at the concept architecture in order to achieve a c_d of 0.25.

3. LITERATURE REVIEW

3.1. PRINCIPLE AND FUNDAMENTALS OF AERODYNAMICS

To analyse and understand vehicle aerodynamics some basic concepts of fluid mechanics and dynamics are necessary, since any vehicle, when in motion, is subjected to an air flow around and through itself.

3.1.1. STREAMLINES

Streamlines are curves associated with a pictorial representation of air flow and are used to study it.

Streamlines are defined as imaginary lines across which there is no flow. If the flow is steady they also indicate the instantaneous direction of the flow and the path that an air particle would follow. For most types of road vehicle there are usually regions of unsteady flow. (Barnard, 2009).

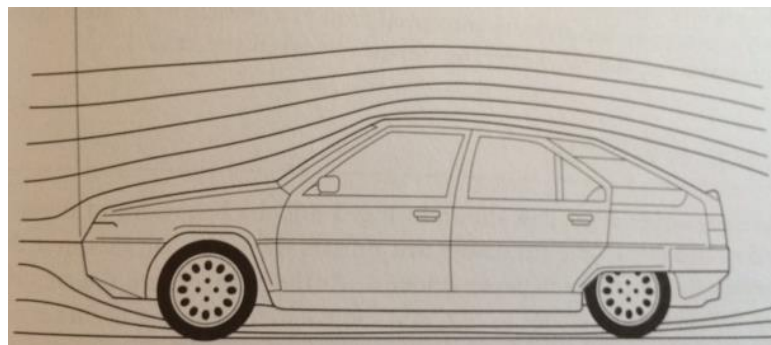


Figure 1- Streamlines (Barnard, 2009)

3.1.2. BOUNDARY LAYERS

An important feature of the flow past a vehicle is that the air appears to stick to the surface. Right next to the surface there is no measurable relative motion (Barnard, 2009).

The thickness of the boundary layer grows with distance from the front of the vehicle, but does not exceed more than a few centimetres on a car travelling at normal open-road speeds. Despite the thinness of this layer, it holds the key to understanding how air flows around a vehicle, and how the lift and drag forces are generated (Barnard, 2009).

There are two different types of boundary layer flows that will be explained ahead.

3.1.3. LAMINAR AND TURBULENT FLOWS

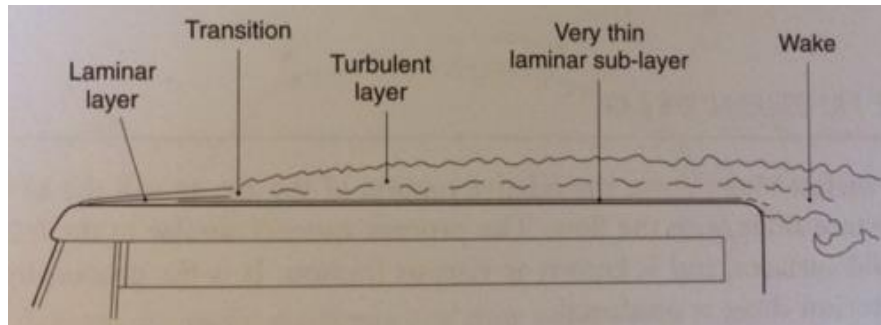


Figure 2- Boundary Layers (Barnard, 2009)

Generally, boundary layers flows are divided into Laminar and Turbulent Flows. Laminar flows have the ideal aerodynamic properties, since fluid motion is well organized with parallel velocity vectors. This kind of flow occurs near the front edge of the vehicle, where the air flows smoothly with no turbulent perturbations.

Further along the vehicle surface, there is a sudden transition to a turbulent flow, in which a random motion appears. In a turbulent flow the organization of velocity vectors cannot be defined.

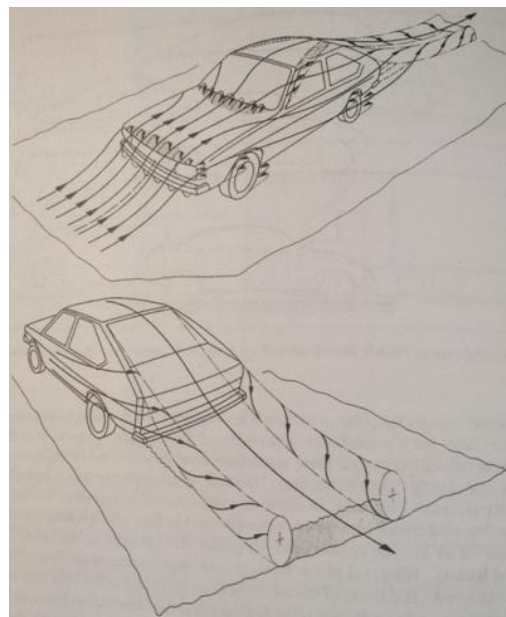


Figure 3- Flow around a Passengers Car (Ahmed et al, 1998)

3.1.4. FLOW SEPARATION

It is important to distinguish between turbulent boundary layer flow and separated flow. In a turbulent boundary layer, the flow is still “streamlined” in the sense that it follows the contour of the body. The turbulent motions are of very small scales. A separated flow does not follow the contours of the body (Barnard, 2009).

Flow separation occurs when the boundary layers travels far enough against an adverse pressure gradient, in other words, when the static pressure increases in the direction of the flow and consequently the velocity decreases. The flow is said to be separated from the surface when velocity is reduced to zero or even become reversed. Flow separation modifies the pressure distribution along the surface and hence the lift and drag characteristics, which will be mentioned ahead.

3.1.5. REYNOLDS NUMBER

The types of boundary layers flows can be defined mathematically by using Reynolds Number value. This is a dimensionless number that can indicate the nature of the flow, as it relates pressure, speed, density, viscosity and the geometry of the body. All of these factors mentioned can modify the behaviour of the layer flow. Reynolds number is given by:

$$Re = \frac{\rho v l}{\mu}$$

where ρ is fluid density, v is the velocity, l is the length of the body and μ is the fluid viscosity. A higher value of Reynolds number indicates turbulent flow while a lower level indicates laminar flow.

3.1.6. DRAG AND LIFT FORCES

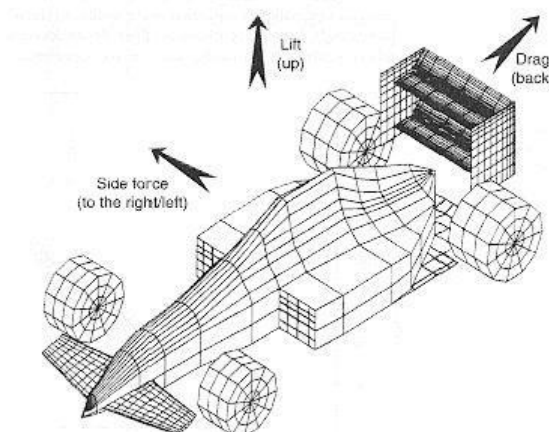


Figure 4- Aerodynamic Forces (Accessed in <http://www.kasravi.com/cmu/tec452/aerodynamics/VehicleAero.htm>)

When a car is travelling, it is moving through an air flow. It is known that it takes some energy to move the car through the air. This energy is used to overcome the **drag**. The

drag force is primarily composed by two forces: the Frontal Pressure and the Rear Vacuum (where the flow detachment or separation occurs).

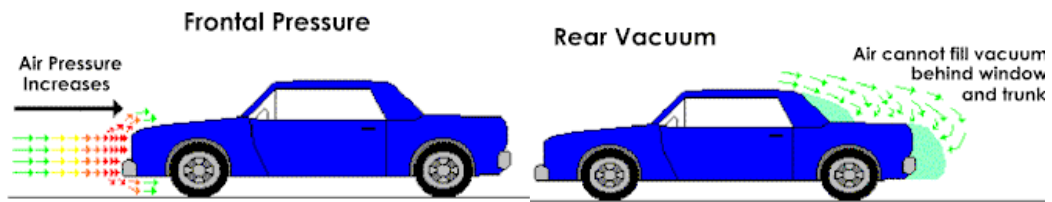


Figure 5- Drag Forces (Accessed in <http://www.up22.com/Aerodynamics.htm>)

Another important force has to be considered in aerodynamic analysis: the Lift Force or Down Force (Negative Lift Force). The lift forces are “created” by low pressure areas (where the flow normally separates) around the surface of the vehicle, while down force is “created” by higher pressure areas.

Lift indirectly affects the drag, but more significantly, considerable improvements in the roadholding and stability can be obtained by reducing the lift, or even generating down force (Barnard, 2009).

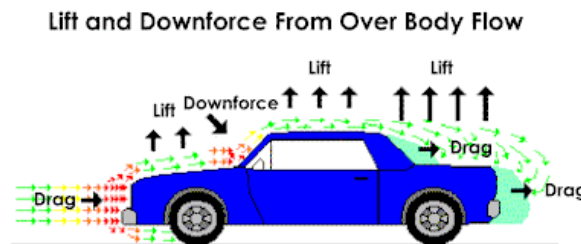


Figure 6- Lift Forces (Accessed in <http://www.up22.com/Aerodynamics.htm>)

3.1.7. DRAG AND LIFT COEFFICIENTS

Drag coefficient (C_D) is used to compare aerodynamic drag produced by vehicles and is dependent on the shape of the vehicle, the frontal area and the speed at which the vehicle is travelling at (Vasiu et al, 2013).

The relationship between drag and these factors can be expressed by:

$$C_D = \frac{D}{\frac{1}{2}\rho V^2 A}$$

Where A is the projected frontal area, ρ is the density of the air, V is the speed of the vehicle relative to the air and D is the drag force.

Minimising the frontal area of the vehicle will minimise the overall drag coefficient of the vehicle. Therefore keeping the vehicle compact and low to the ground as possible will give low frontal projected area value for the vehicle and therefore better performance (Vasiu et al, 2013).

Lift coefficient (C_L) is defined in a similar way to drag coefficient:

$$C_L = \frac{L}{\frac{1}{2}\rho V^2 A}$$

Where A is the projected frontal area, ρ is the density of the air, V is the speed of the vehicle relative to the air and D is the lift force.

3.2. HOW TO IMPROVE AERODYNAMIC PERFORMANCE

3.2.1. WIND TUNNEL TESTING

There are many ways to optimize the aerodynamic performance of a vehicle. The wind tunnel testing is used to analyse aerodynamics and identify low pressure areas and regions that can be modified to improve performance.

The main development device for the vehicle aerodynamics testing continues to be the full-scale wind-tunnel. It is likely that this will be unchanged for many years ahead since there is no reliable alternative for it. There are two main types of conventional wind-tunnels: open jet, which has an open test section, and the second type is a closed wind-tunnel with a closed test section (Le Good, 1998).

3.2.2. DESIGN DEVELOPMENT

During the design development of a car, choosing the front end, rear end, windshield, roof and underbody configurations, for example, can be crucial to the aerodynamic performance of the vehicle. Some of these configurations and how they can improve the aerodynamic performance will be discussed below:

Front End Configuration

The front end is influenced by the bonnet length and windscreen inclination. According to Flegl and Lechner, a low stagnation point offers good possibilities for favourable drag and lift coefficients (Businaro et al, 1983).

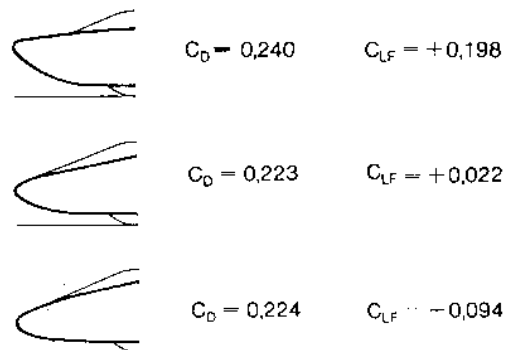
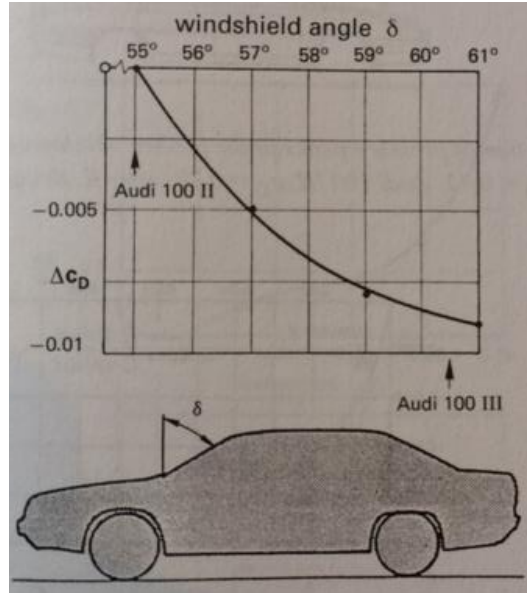


Figure 7- Different front end shapes and drag coefficient (Vasiu et al, 2013)

Windshield and A-Pillar

The next below shows how the windshield inclination influences on drag coefficient of the Audi 100 III Vehicle.



Graph 1- Windshield Angle influences on Drag Coefficient (Ahmed et al, 1998)

Rear End Configuration

There are different types of rear configurations including fastback (or hatchback), notchback and square back (Barnard, 2009).

At the rear of a hatch back there is a region of low pressure, and conical vortices generate due to flow separation from the rear corners, becoming strong trailing vortices (Barnard, 2009).

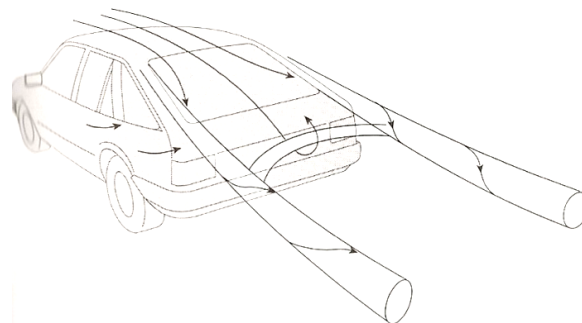


Figure 8- Conical Vortices Generated on Hatchback (Vasiu et al, 2013)

In the case of a rear notch back car, the line joining the rear end of the roofline and the tip of the boot is defined by angle θ_{eff} . As indicated on figure 9, the variation in this angle has similarities to the drag coefficients of a hatchback. This angle relates with the discovery that raising or lengthening the boot would usually reduce drag. When the boot height is raised, θ_{eff} decreases (Barnard, 2009).

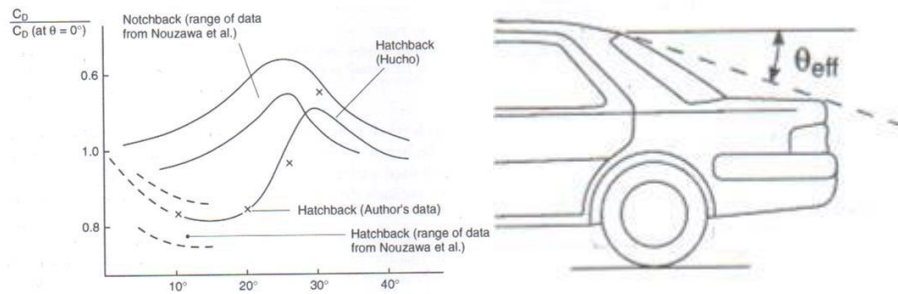
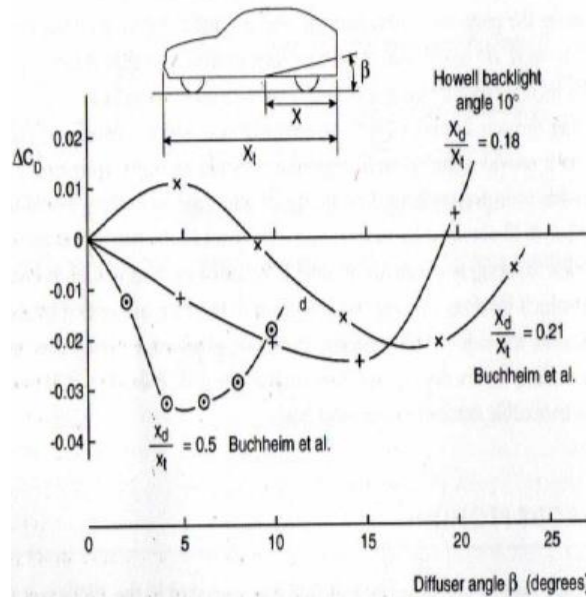


Figure 9- Effective Rear Slope Angle (Vasiu et al, 2013)

Underbody

The drag coefficient can be improved by rising the under floor towards the rear creating a diffuser effect. The diffuser angle (under-body tapering at the rear) and its effects are illustrated in the figure below:

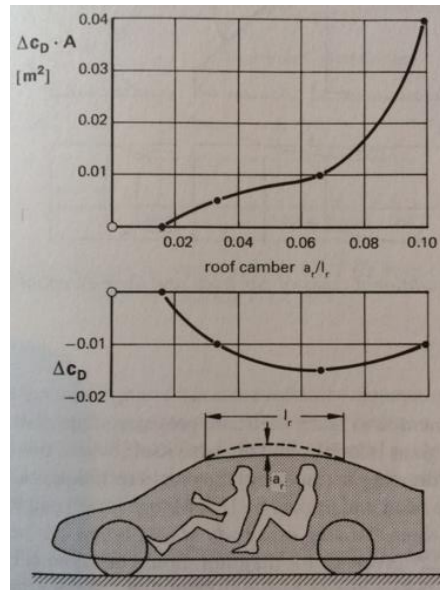


Graph 2- Underbody Diffuser (Barnard, 2009)

Roof

The drag coefficient can be reduced by arching the roof in the longitudinal direction; however if the curvature is too great, C_D again can increase (Ahmed et al, 1998).

However, the design of the roof arch must ensure that the frontal area of a car remains constant; if not, the absolute drag ($C_D \times A$) can increase despite a reduction in drag coefficient, as shown in the upper graph of the next figure (Ahmed et al, 1998).



Graph 3- Roof Shape influences on Drag Coefficient (Ahmed et al, 1998)

3.2.3. DEVICES AND GENERAL IMPROVEMENTS

The next figure illustrates 13 modifications that can be made in a vehicle design to improve aerodynamic performance:

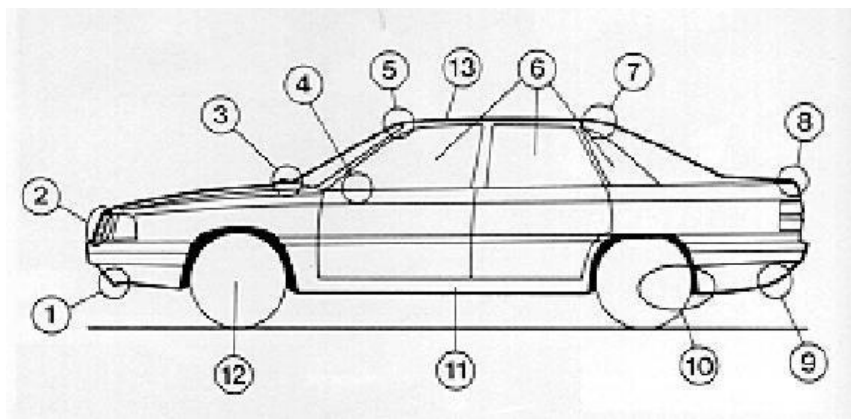


Figure 10- General Improvements (Accessed in <http://www.kasravi.com/cmu/tec452/aerodynamics/VehicleAero.htm>)

1- Front spoiler, 2- Ducted engine cooling; 3- Shrouded windshield wiper arms; 4- Aerodynamic mirrors; 5- Smooth windshield transitions; 6- Smooth side window transitions; 7- Smooth rear window transition; 8- Optimized trunk corner radii; 9- Optimized lower rear panel; 10 - Smooth fuel tank and underbody; 11- Optimized rocker panels; 12- Flush wheel covers; 13- Elimination of the rain gutter.

Spoilers act like barriers to air flow. While rear spoilers are commonly used to create high pressure areas above the trunk of sedan vehicles (These kind of vehicles tends to be lighter in the rear end), front spoilers are used to restrict air flow under the vehicle, consequently reducing pressure under the vehicle and lift forces.

Covering wheels, when permitted by regulations, is a great solution to reduce drag, since open wheels create air flow turbulence and, obviously, increase drag forces.

A vehicle body design needs to be as smooth as possible. A bodywork which quickly converges forces the air flow into turbulence and, as mentioned previously, consequently increases drag forces.

4. TARF-LCV PREVIOUS CONCEPTS CASE STUDY

In order to achieve better results in the Concept #6 CFD simulations (the main focus of this project), it is important to understand the evolution of the project through the previous concepts.

In this section, the design and aerodynamics of previous TARF-LCV concepts will be discussed and analyzed.

4.1. CONCEPT #1



Figure 11- TARF-LCV 1st concept

The first concept design was mainly focused in minimizing drag effects. It was designed with the aid of design hub, to give the TARF new and attractive design features. This was to give the concept a futuristic design that may be a vision in 20 years also providing an aesthetically pleasing design which satisfy this requirement of the customer (Vasiu et al, 2013).

4.1.1. CHARACTERISTICS

- Front-end:
 - Windscreen inclination angle: 65°;
 - Bonnet wedge angle: 13°;
 - Bonnet height: 650mm;
 - Bonnet radius;

- Bumper and front wheel arches – curvy design to direct the air flow as recommended from product analysis and maintain flow attachment;
- Head lights design being integrated;
- Extended front wheel arch covers;
- Rear-end:
 - Rear Rake angle: 25°;
 - Spoiler;
 - Rear wheel fairing;
- Passengers compartment area;
- Side body streamlining;
- Wheel size: 205/55/R17;
- Frontal area.

4.1.2. AERODYNAMIC ANALYSIS

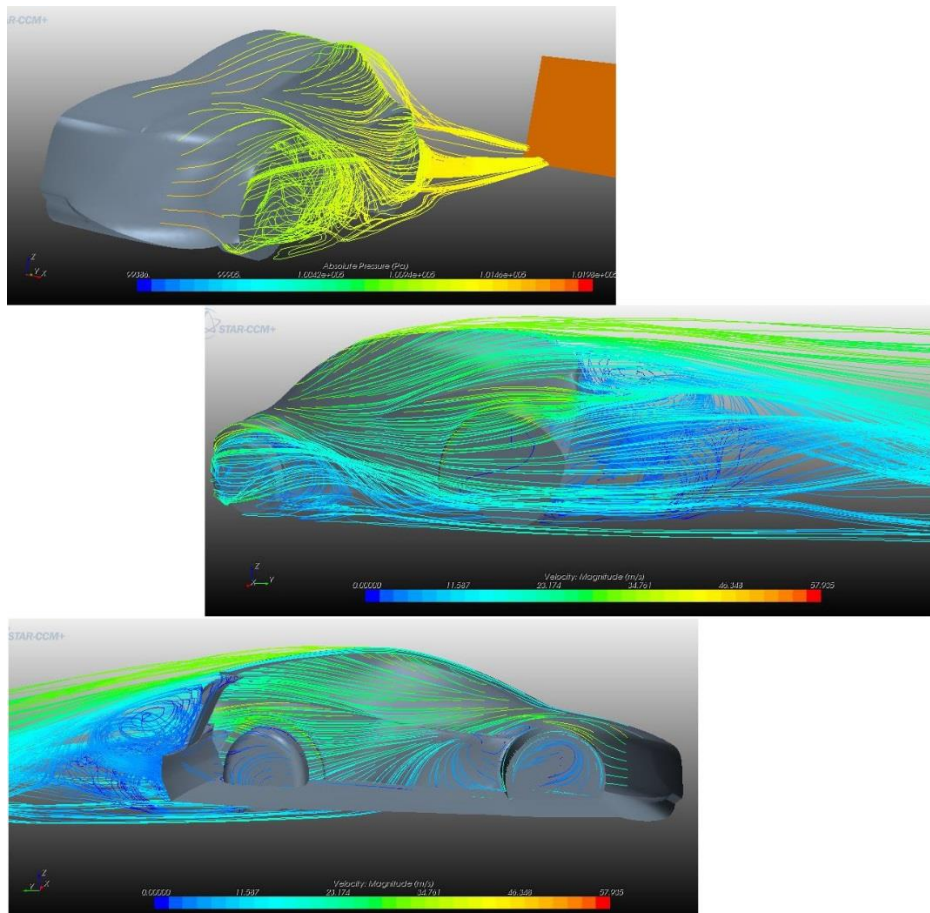


Figure 12- Concept #1 Streamlines

The CFD analysis of Concept #1 returned the following results (at an average speed of 32 m/s):

Frontal Area	Drag Coefficient	Lift Coefficient
2.4 m ²	0.327	0.113

Table 1- Concept #1 CFD Results

The figure below shows the pressure distribution over the vehicle. Regions in red color refers to high pressure areas, where stagnation points are positioned. Blue regions illustrate low pressure areas.

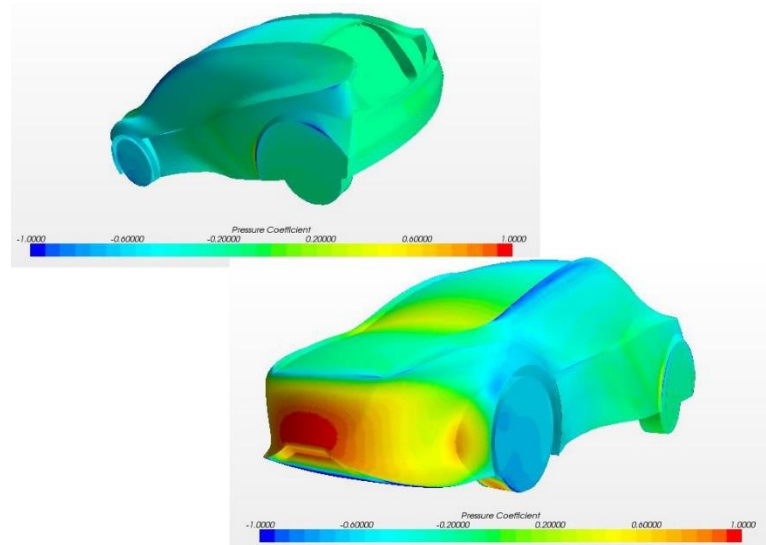


Figure 13- Concept #1 Pressure Coefficient

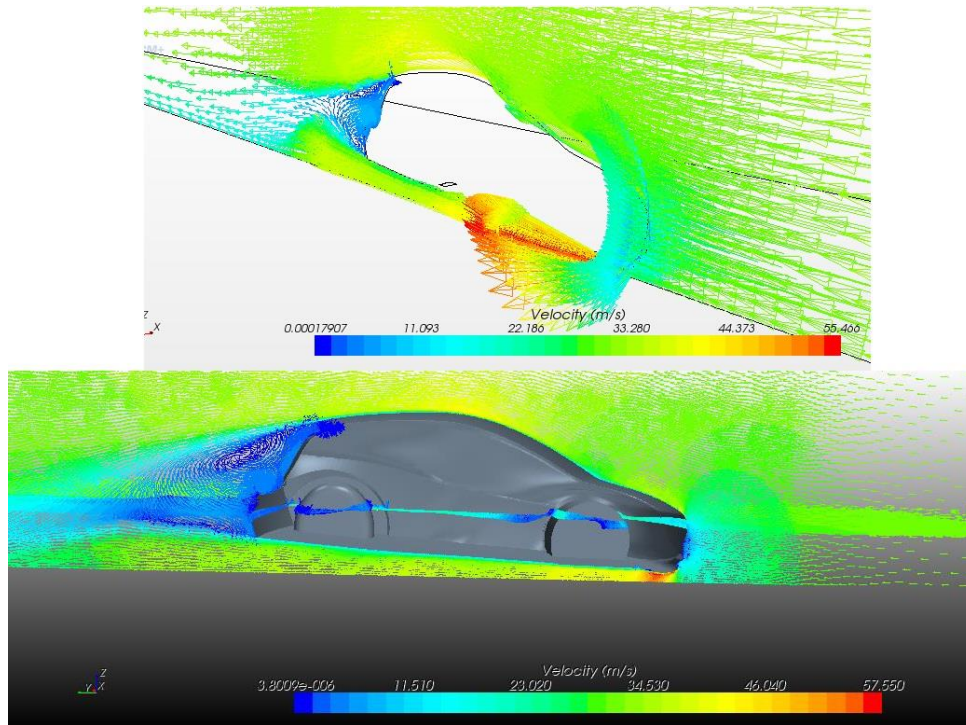


Figure 14- Concept #1 Velocity Field

Figure 14 shows the flow characteristics at a speed of 32m/s. The region at the rear of the vehicle shows vortex and turbulent wake being generated when the flow separates. Front-end region shows flow separation, and a trailing vortex is generated at the top of the model. (Vasiu et al, 2013)

4.2. CONCEPT #2

After running some CFD simulations on the concept #1, some refinements were made on TARF's architecture design, in order to obtain a better aerodynamic performance.

4.2.1. MODIFICATIONS

- Front end:
 - Bumper - smoothen edges on front;
 - Bonnet height – pedestrian safety and aerodynamic requirement;
 - Bonnet curvature;
- Rear configuration:
 - Rake angle - reduce from 25° to 18°;
 - Spoiler – removed to give smoother longer extended roof surface to maintain the new rake angle of 18°;
 - Bumper;
 - Tailgate design;
- Pillar recess from front to the rear of the vehicle;
- Smooth rounded edges on side body including wheel fair and front and rear arches;

- Transition of side body smoother - front occupants compartment door region wider;
- Side streamlined;
- Frontal areas reduce.

The front bumper and bonnet design of the model was refined to provide smoother edges and transition by increasing the radius of the surface, including the feature on the low region of the front bumper, and lowering the lip feature (Vasiu et al, 2013).

The following images demonstrates the modifications made on the front-end, side body and rear-end, respectively:

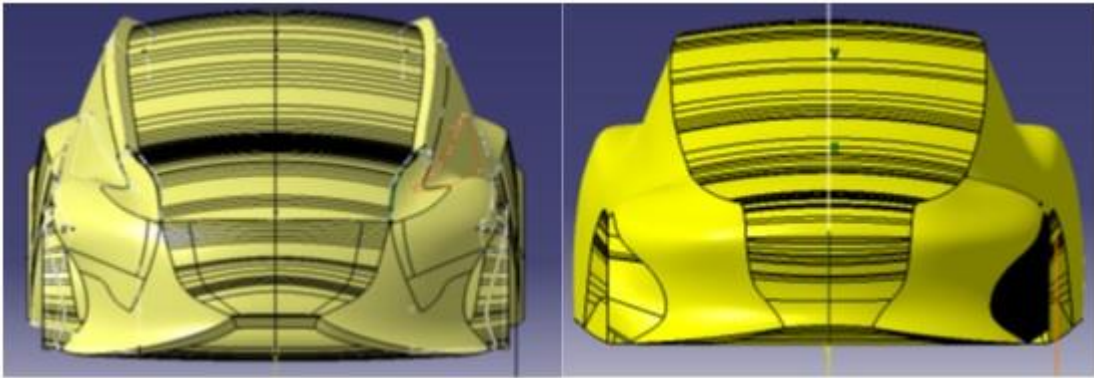


Figure 15- Concepts #1 and #2 Front-end

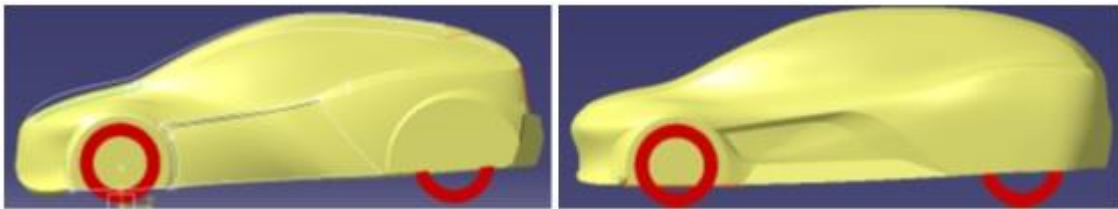


Figure 16- Concepts #1 and #2 Side body

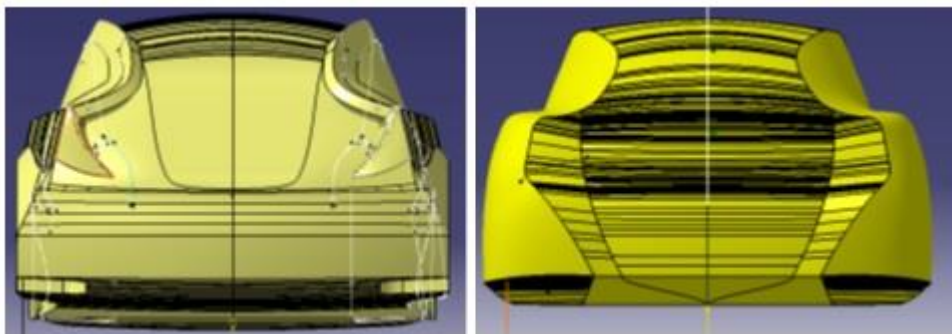


Figure 17- Concepts #1 and #2 Rear-end

All modifications made to the model were mainly focused on increasing aerodynamic performance. However, a few changes were made to meet some regulations. It includes an approach and departure angles on the bumpers, to ensure that they don't touch the floor when going through bumpers or stepped roads, for example. Changes were also made on the A-pillar and in the tailgate so that driver's visibility was

improved. Modifications to side body and rake angle increased occupant's compartment, providing more comfort to them.

4.3. CONCEPT #3

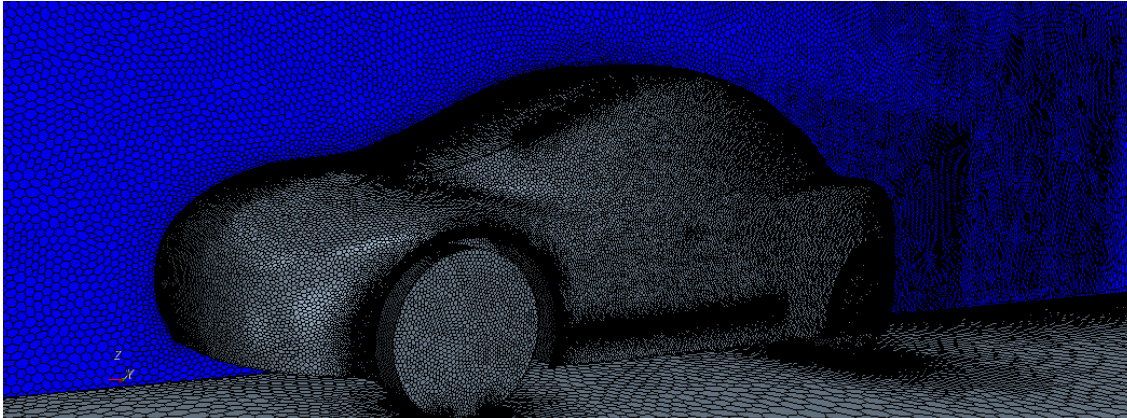


Figure 18- Concept #3 Mesh Scene

Overall there were a few discrepancies with concept model #2 from the designer (due to design for aesthetics and styling) including the headroom space at the rear passenger's compartment. The ground clearance height was not maintained all the way to the rear of the vehicle. These would need to be refined in the next iteration for concept #3 to provide better aerodynamic performance (Vasiu et al, 2013).

4.3.1. MODIFICATIONS

In comparison to the previous model, the following modifications were made on the third concept of TARF:

- Front end:
 - Added volume, and rounded front bumper with smoother transition between bumper and wheel arch – gives more packaging space as well;
 - Bonnet space – for packaging of components;
- Rear end:
 - Extended rake angle of 12.5° (ideal rear rake angle) - as reviewed from the Mira reference car & Remus;
 - Reduced the width of the rear arch (shoulder) also providing a side tape;
 - Diffuser angle;
- Head room space for manikins – more room added;
- Volume added to side body sill section – more flushed for aero and more occupant's compartment space;
- Rounded edges of the models pillar up to the rear of the vehicle (Vasiu et al, 2013).

The modifications aforementioned are shown in the figures below. The front-end, side body and rear-end of both vehicles are presented, respectively. The vehicle on the left side is Concept #2, while Concept #3 is on the right side.

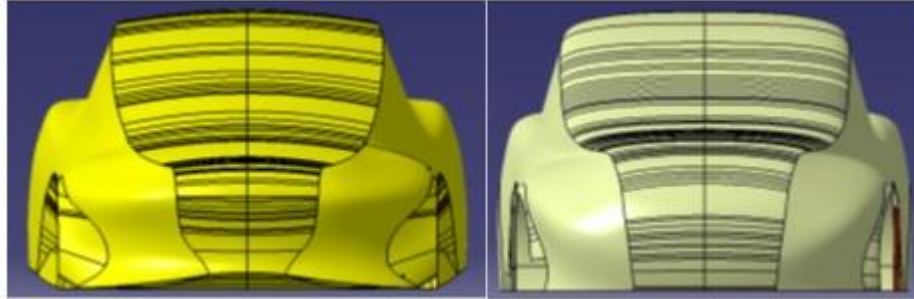


Figure 19- Concepts #2 and #3 Front-end

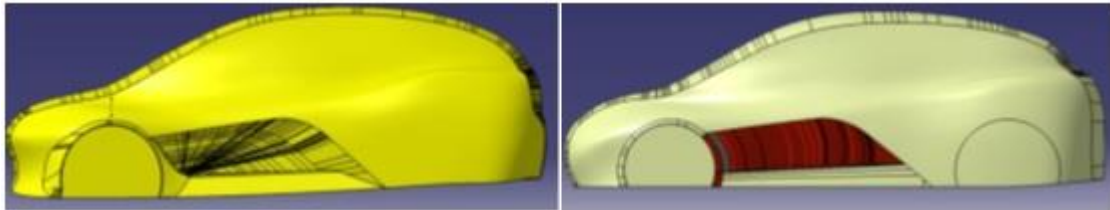


Figure 20- Concepts #2 and #3 Side body

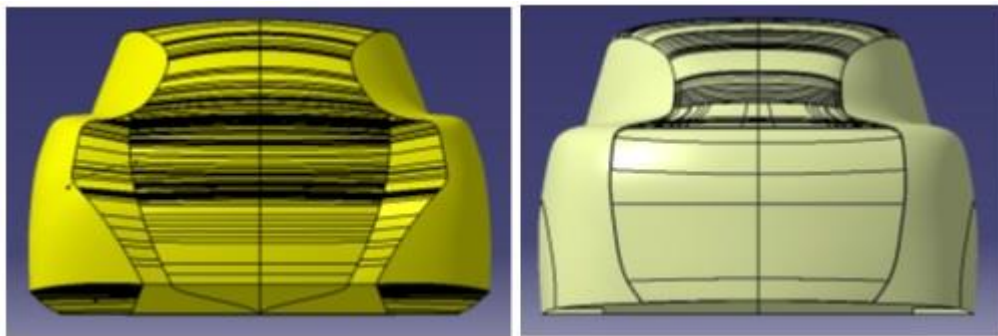


Figure 21- Concepts #2 and #3 Rear-end

4.3.2. AERODYNAMIC ANALYSIS

Results obtained on CFD analysis of Concept #3 are shown on the following table and figures:

Drag Coefficient	Lift Coefficient
0.29	0.32

Table 2- Concept #3 CFD Results

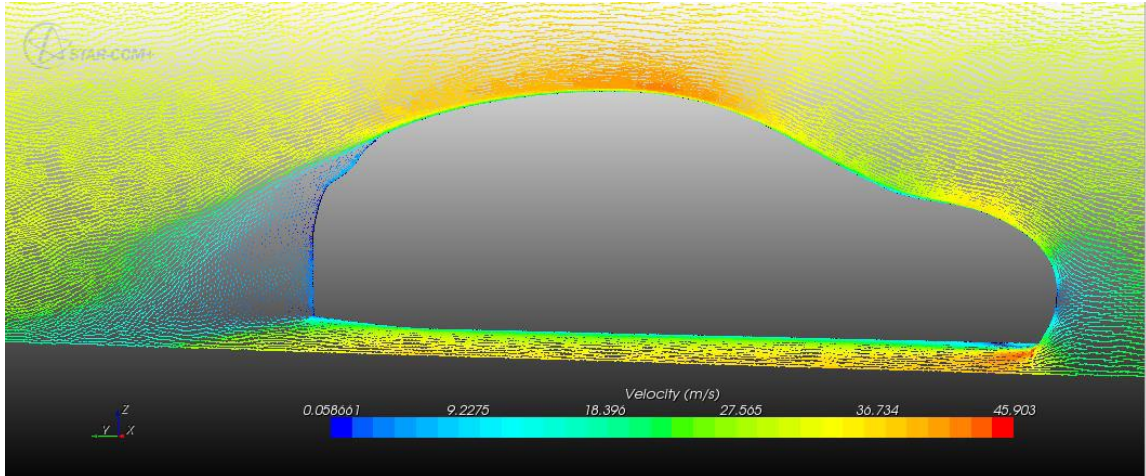


Figure 22- Concept #4 Velocity Field

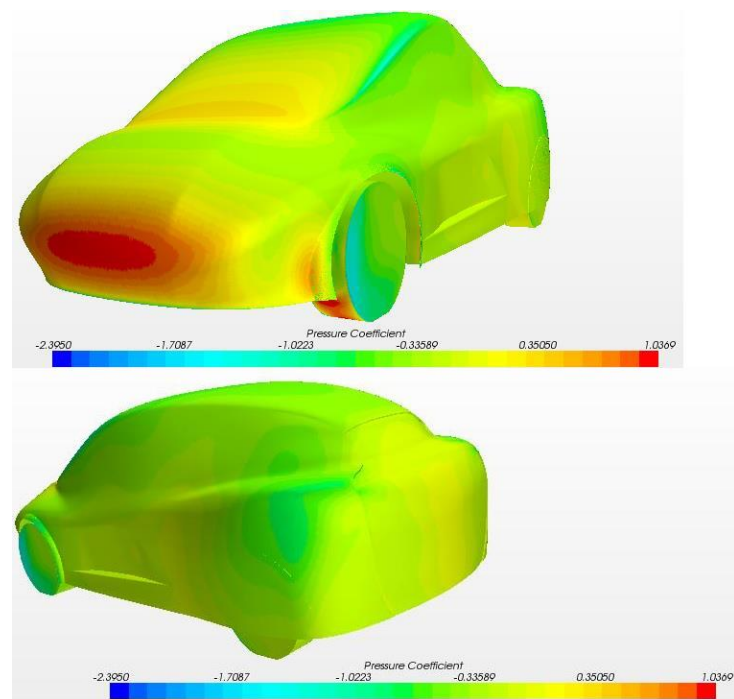


Figure 23- Concept #4 Pressure Coefficient

Figure 22 shows the flow visualization, while figure 23 shows the pressure distribution around the vehicle surface.

4.4. CONCEPT #4

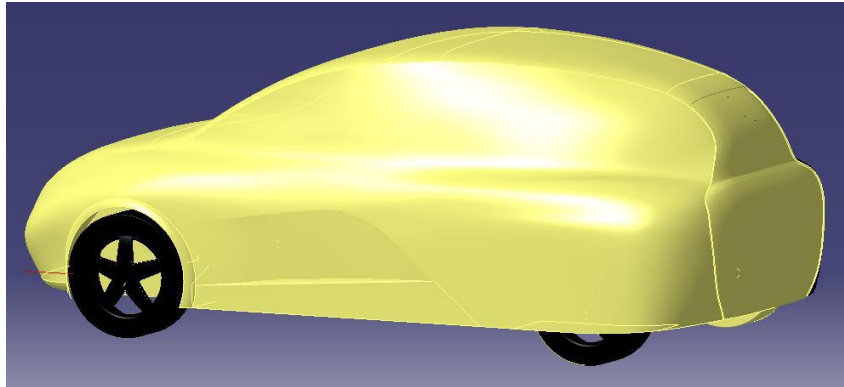


Figure 24- Concept #4 Final Design

4.4.1. MODIFICATIONS

Provided that the target for the drag coefficient for the fourth model was 0.28, there weren't too much changes in comparison to the third model, since the previous achieved a 0.29 drag coefficient.

Basically, these were the changes:

- Overall width was decrease from front and rear hence reducing the frontal area;
- The frontal arch/fender's volume was increased;
- Front bumper splitter was rounded.

4.4.2. AERODYNAMIC ANALYSIS

After another CFD simulation was carried out, Concept #4 achieved the following results, at 32 m/s:

Drag Coefficient	Lift Coefficient
0.27	0.30

Table 3- Concept #4 CFD Results

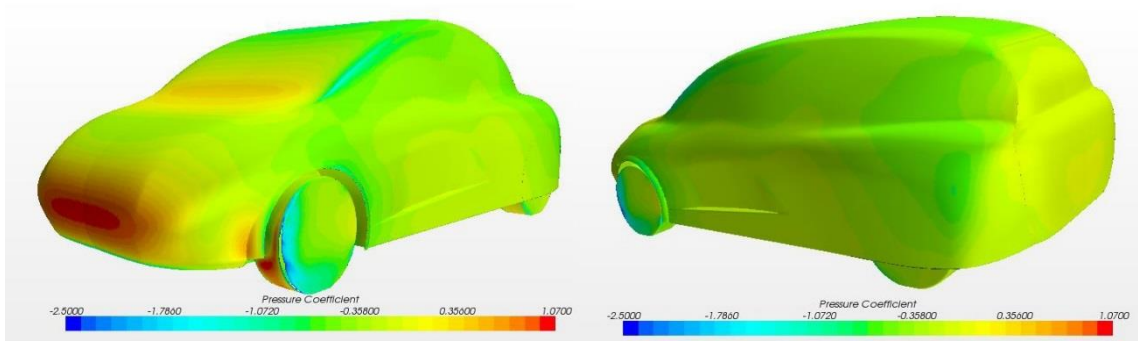


Figure 25- Concept #4 Pressure Coefficient

Red regions on the figure above shows stagnation pressure, while blue regions represents low pressure areas, where the flow separates. Red region on wheels occurs because wheels are slightly exposed.

Figure 26 demonstrates flow behaviour around the vehicle surface.

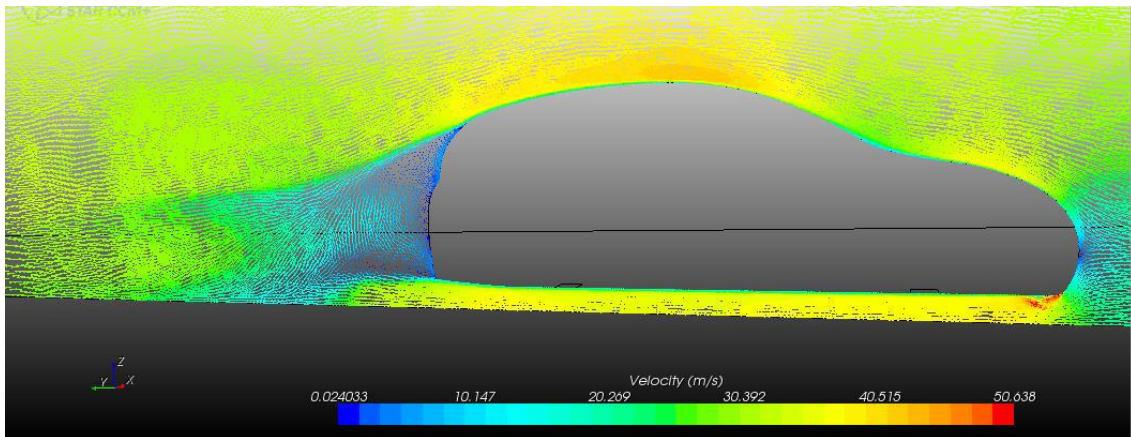


Figure 26- Concept #4 Velocity Field

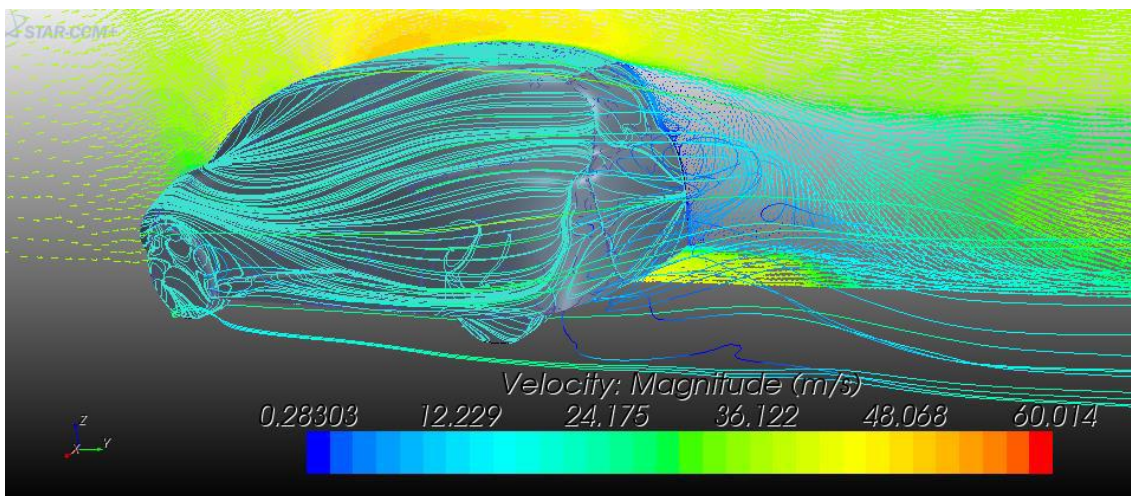


Figure 27- Concept #4 Streamlines

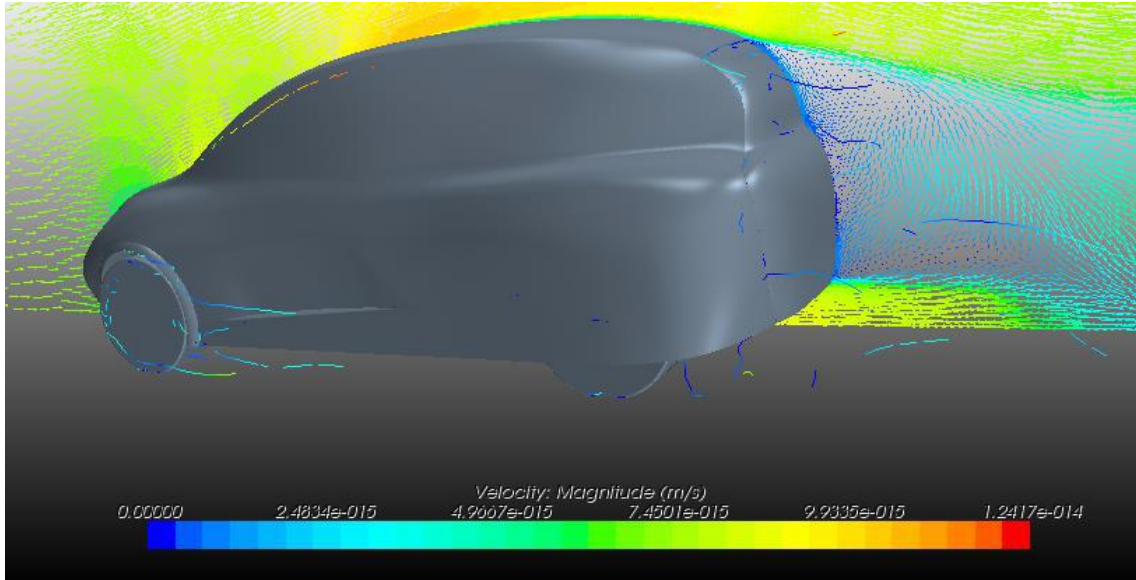


Figure 28- Vortex Core and Flow Separation

Figures 27 and 28 illustrates flow attachment and separation and also wake formation around the vehicle.

All information regarding Concepts number 1 to 4 presented in this Case Study were taken from the “*TARF-LCV Product Innovation*” project report, from Coventry University (2013).

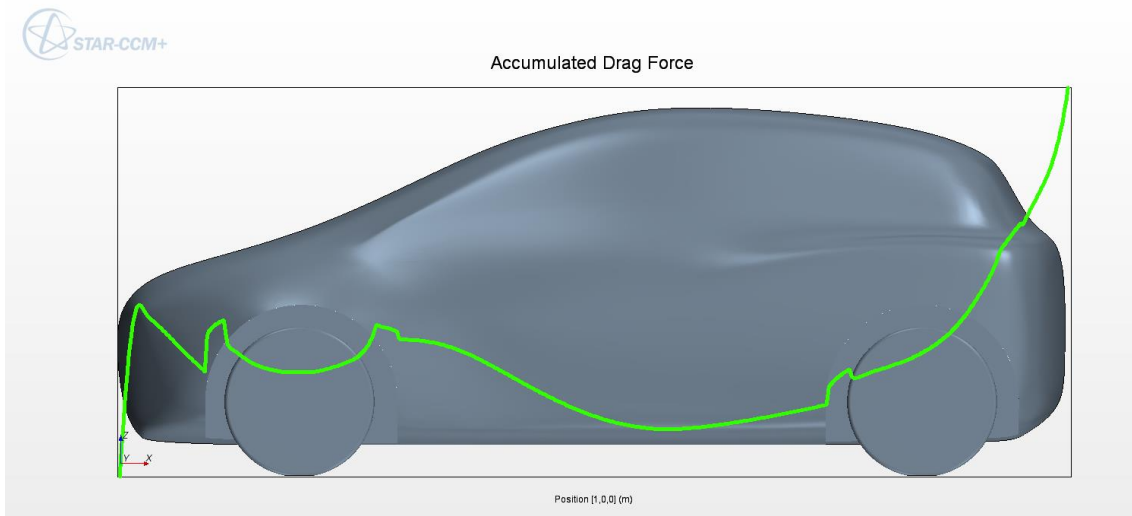
4.5. CONCEPT #5

Information about the fifth model are scarce, but it is known that the drag coefficient has increased in comparison with previous model. It is also known that lift force in the rear-end is considerably greater than in the front-end.

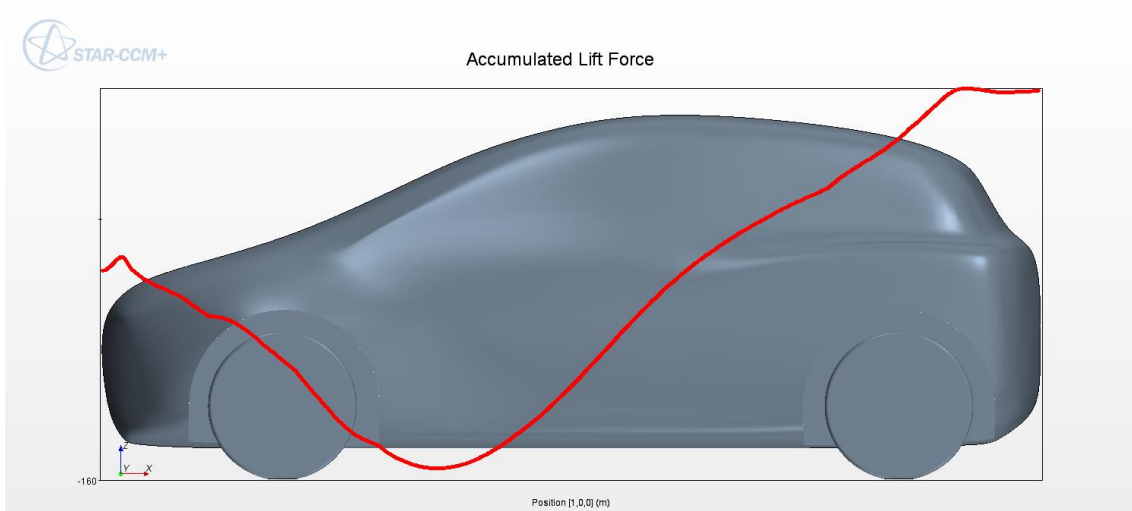
Following table and graphs illustrates this information:

Drag Coefficient	Lift Coefficient - Front	Lift Coefficient – Rear
0.31	0.03	0.2

Table 4- Concept #5 CFD Results



Graph 4- Concept #5 Drag Force Distribution



Graph 5- Concept #5 Lift Force Distribution

5. METHODOLOGY – MODELLING THE CONCEPT #6 CFD SIMULATION

Modelling a CFD simulation is the most important task when analysing the aerodynamic performance. Any mistake made during modelling can influence the outcome results, as will be shown later on.

The CAD model was imported from CATIA as .stl file in STAR-CCM+, and the first was to check the geometry surface and repair it. The under body surface manipulations were done as the surfaces were not closed on either sides. A New surface was made for half of the vehicle body making a contact with the adjacent surfaces. The created surface was mirrored with XY plane as reference plane.

All parts of the geometry were assigned to one part using the *Combine* operation. The combined part was then assigned to a region using the option “Assign parts to regions”. A region was created to apply surface meshing. To remove all the free edges, non-manifold edges and non-manifold vertices surface meshing needs to be done. The two options available for meshing were *Surface Remeshing* and *Surface Wrapping*. The surface remesher will increase the surface quality by re-arranging the triangles. But it cannot be done for a closed surface. Surface wrapping allows the part to be a closed surface, but the surface quality might not be increased or may have poor surface quality. So, surface wrapper was selected to have a closed surface.

The Surface Wrapper tool was created after assigning the geometry parts to regions (1 region per part and 1 boundary per part surface). Surface Wrapper properties are shown below:

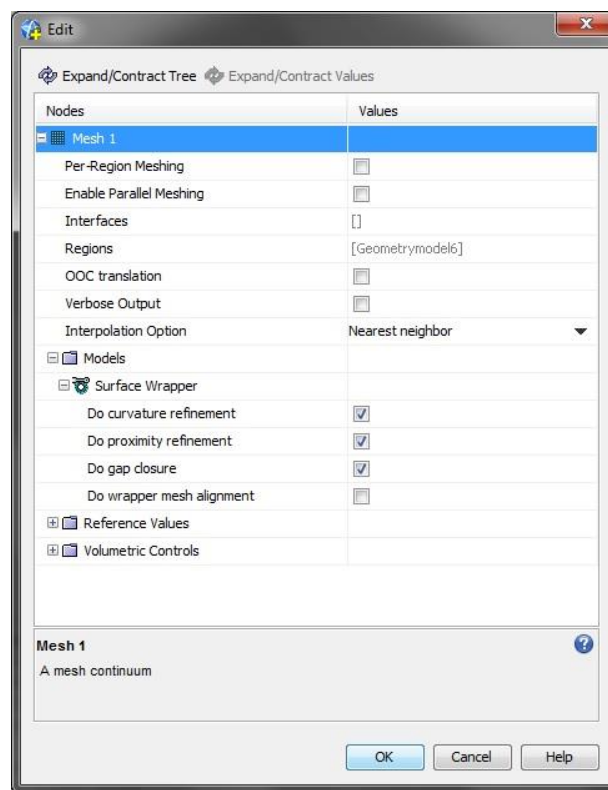


Figure 29- Surface Wrapper Properties

After the repair tool was activated, the surface was checked again. The result is presented in Figure 30.

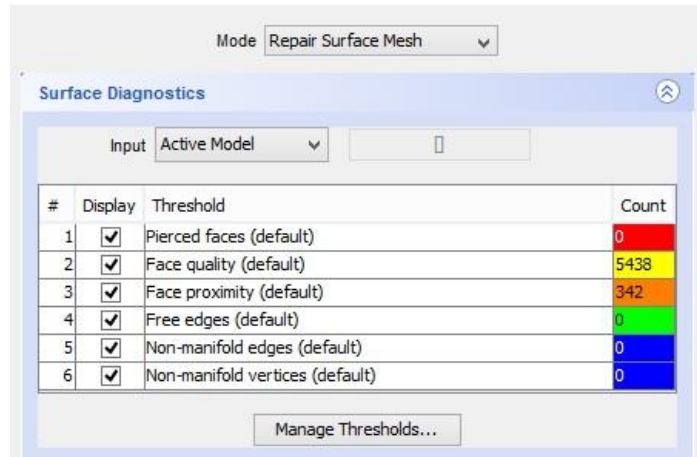


Figure 30- Surface Diagnostic

It's important to remember that not all fields need to be equal to zero, however the STAR-CCM+ Auto Repair tool was used to do so.

Next step was to create the wind tunnel. Using STAR-CCM+ CAD features, a block was created around the left half of the vehicle, considering the vehicle symmetry (the computation will be easier), as shown below:

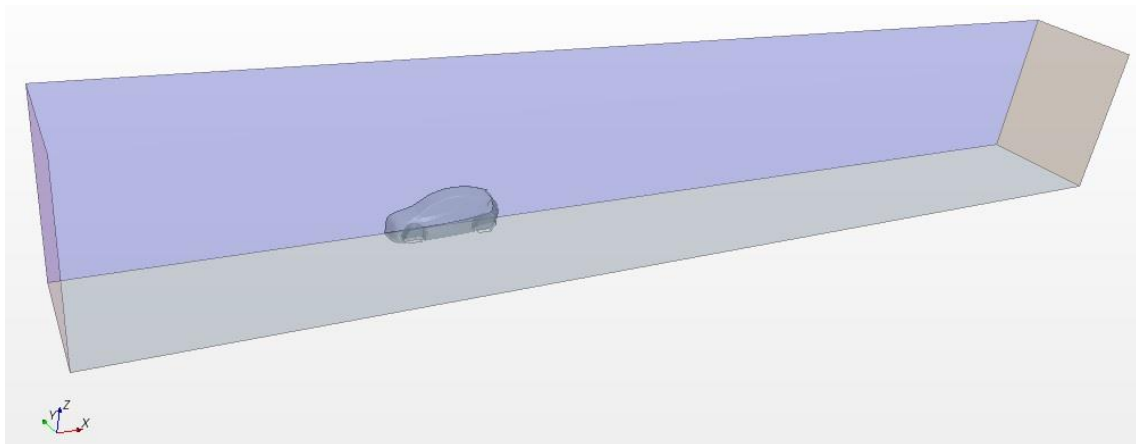


Figure 31- Wind Tunnel

After that, the block surface was split by patch, creating the inlet, outlet, floor, walls and symmetry surfaces.

Then, the vehicle surface was subtracted from the block (wind tunnel), creating a new part called "Subtract", and the "Subtract" surfaces were assigned to regions.

Subtract regions received the following properties:

Region	Type
Inlet	Velocity Inlet
Outlet	Pressure Outlet
Symmetry	Symmetry Plane

Table 5- Wind Tunnel Regions Properties

Next step was to create 2 Volumetric Controls around the vehicle. A volumetric control allows you to refine or coarsen the mesh density for a surface and/or volume mesh, based on a volume shape (CD-adapco, 2013).

Next task was to set up a new Mesh Continuum. The following mesh models were selected:

- ❖ Polyhedral Mesher;
- ❖ Prism Layer Mesher;
- ❖ Surface remesher.

Various options for volume meshing were available. Polyhedral mesher was selected as it produces easy and balanced solution to typical geometrical shapes. It is much better than tetrahedral mesher in terms of cell productivity as the polyhedral mesh produces fewer cells comparatively. Prism layer mesher was used in combination of polyhedral mesher to improve the accuracy of the solution as it helps in settling the turbulent boundary layer. Embedded thin mesher is selected for creating cells for thin geometry as the vehicle has fins over the head lights and the wheel arches which were considerably thin when compared to the vehicle body. Base size, polynomial density and polynomial volume density were manipulated to have a good volume mesh.

Table 6 shows the reference values used:

Base Size	Different Values were used
Surface Size	Relative Minimum Size: 25% of base
	Relative Target Size: 100% of base
Number of prism layers	6
Prism Layer Thickness (Absolute Size)	10 mm
Surface Growth Rate	1.1

Table 6- Mesh Continuum Reference Values

As table 6 shows, different values were used in different simulations for the base size.

It is also important to remember that specific surface sizes were used for the vehicle:

- ❖ Relative Minimum size: 1.5% of base size;
- ❖ Relative Target size: 7.5% of base size.

The “Customise Prism Mesh” feature was disabled for the floor and walls.

From this point, Surface and Volume meshes can be generated, however it was decided to set up the Physics before generating it.

Physics models selected were:

- ❖ Three Dimensional Flow;
- ❖ Steady flow;
- ❖ Working Fluid – Gas (air);
- ❖ Segregated flow;
- ❖ Constant Density;

- ❖ Turbulent;
- ❖ K-Epsilon turbulence;
- ❖ Two Layer All y+ treatment;
- ❖ Cell Quality Remediation.

There were a lot of options available for setting up the physics using physics continua. **Three dimensional model** was selected as the mesh was a three dimensional mesh. **Steady model** was selected under time modelling as to have calculations under steady state. In material modelling single component **gas model** has been chosen as the input is air. **Segregated flow model** was selected as it would consume less computing memory for respective algorithm. **Turbulent modelling** was chosen as the Reynolds number value was seen the region where the turbulent flow is seen. **K-epsilon turbulence model** was also selected as it quantifies turbulent kinetic energy and respective dissipation rate. In this model realizable K-Epsilon two layer model and **two layer All y+ wall treatment** have been chosen automatically. **Cell quality remediation** was chosen to avoid poor quality cells and tries to improve the solution nearer to accuracy based on the mesh quality.

Some Physics conditions were also set before running simulation. For the Floor and Walls regions, the Shear Stress Specification method was set to “Slip” and for the Inlet region the initial velocity magnitude was set to 32 m/s (in direction of flow).

Frontal Area, Drag and Lift Coefficients Reports were also created, using 32m/s as Reference Velocity and 1.18415 kg/m³ as Reference Density.

From this point, the simulation model is ready to run.

However, before running the simulation, reports were created: frontal area and force coefficients (drag and lift). The drag coefficient and lift coefficient were added to the monitors so that, for every iteration coefficients would be observed and necessary steps could be taken under bad results. Lift and drag coefficients were also added to plots for which the plot will be made with the iterations. Number of iterations was changed to save time as the values gets stabilised. Run control was used to start the iterations.

It is important to remember that the simulation can be stopped when it converges, and according to CD-adapco, STAR-CCM+ software developer, the case is considered as converged if:

- ❖ Residuals have dropped 2-3 orders of magnitude;
- ❖ Engineering quantities of interest have stopped changing.

After about 2200 iterations, simulation was stopped and post processing was done to understand the aerodynamics of the vehicle. Scalar scenes like pressure coefficient, total absolute pressure and velocity magnitude were used to understand the pressure points on the vehicle during the CFD analysis. Vector scenes like velocity around the vehicle and tangential velocity on the floor were used. Stream line scenes were created around the vehicle to understand the flow of the air around the vehicle. Iso-surfaces were created for total pressure to demonstrate the wake around the vehicle.

The results of post processing analysis will be shown in the next section of this report.

6. CONCEPT #6 – CFD RESULTS

As reported before, more than one simulation was created for the geometry, with different base sizes for the volume meshing, and also with 2 different distances between the floor and the vehicle, as figure 35 will show. In this section the results of the simulations will be described.

Four simulations were created with a lower distance between the vehicle and the floor, using different base sizes for the volume meshing. The Frontal Area of the vehicle in these simulations was 1.074 m².

The following table shows the results:

Base Size of Volume Meshing	Drag Coefficient
1500 mm	0.316
600 mm	0.296
450 mm	0.283
300 mm	0.269

Table 7- Base Sizes and CFD Results

Mesh scenes are available in the Appendix.

After this simulations, it was realized that the distance between vehicle and floor was **wrong**, since the vehicle was too close to the floor surface and it was not representing the reality.

Therefore, another simulation with a different distance between vehicle and floor was created, with a Volume Meshing base size of 300 mm. Results are shown above:

Frontal Area	Drag Coefficient	Lift Coefficient
1.099 m ²	0.287	0.067

Table 8- Concept #6 CFD Results

```

: Output
tarf#6 simulation_Copy x Drag Coefficient Report x
Normal [ 1.000000e+00, 0.000000e+00, 0.000000e+00] (in Lab Coordinate System)
Viewup [ 0.000000e+00, 0.000000e+00, 1.000000e+00] (in Lab Coordinate System)

Parts
-----
Model for Remus.catia
-----

Total                                1.099143e+00 (m^2)

```

Figure 32- Frontal Area Report

Output			
tarf#6 simulation_Copy x		Drag Coefficient Report x	
Part	Pressure ()	Shear ()	Net ()
Model for Remus.catia	2.681595e-01	1.959284e-02	2.877523e-01
Totals:	2.681595e-01	1.959284e-02	2.877523e-01
Monitor value: 0.2877523342494918			

Figure 33- Drag Coefficient Report

Output			
tarf#6 simulation_Copy x		Lift Coefficient Report x	
Part	Pressure ()	Shear ()	Net ()
Model for Remus.catia	6.398750e-02	3.065811e-03	6.705331e-02
Totals:	6.398750e-02	3.065811e-03	6.705331e-02
Monitor value: 0.06705330775201411			

Figure 34- Lift Coefficient Report

Figure 35 shows both distances between the vehicle and the floor:

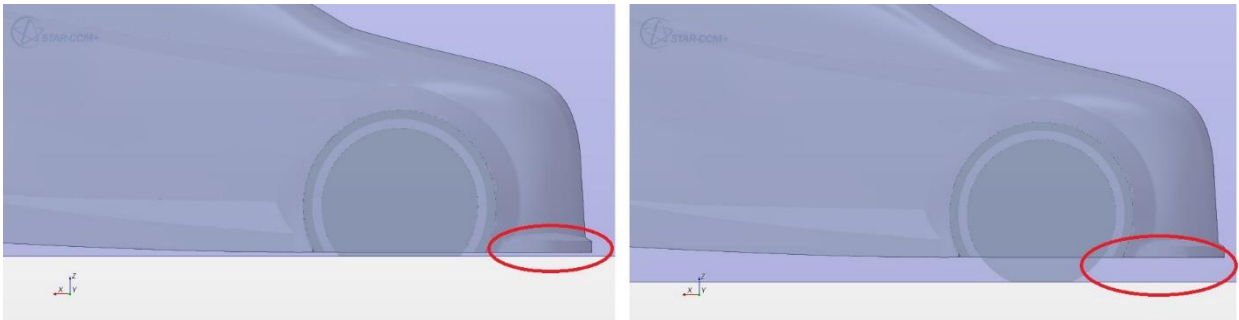
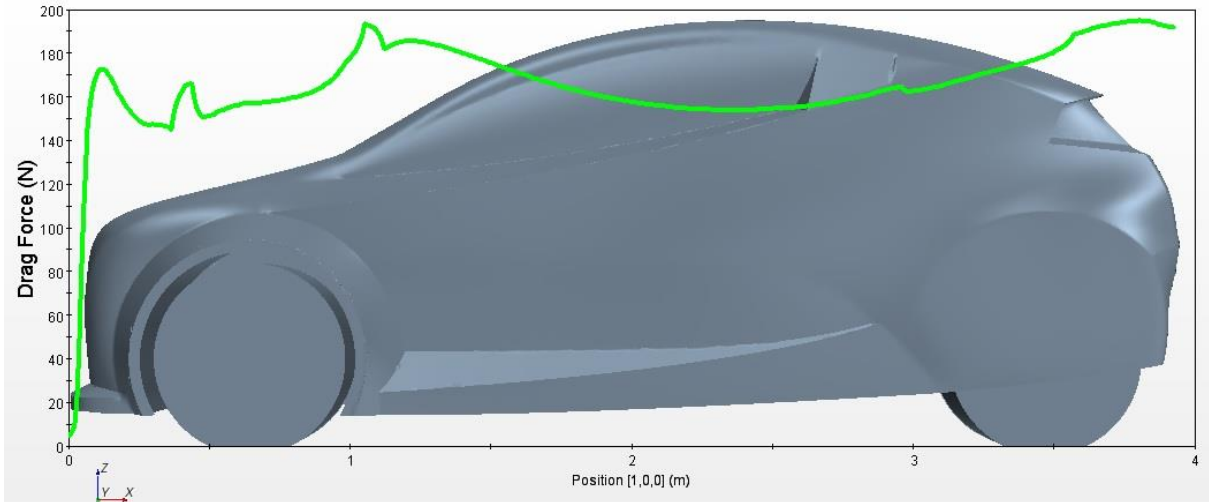


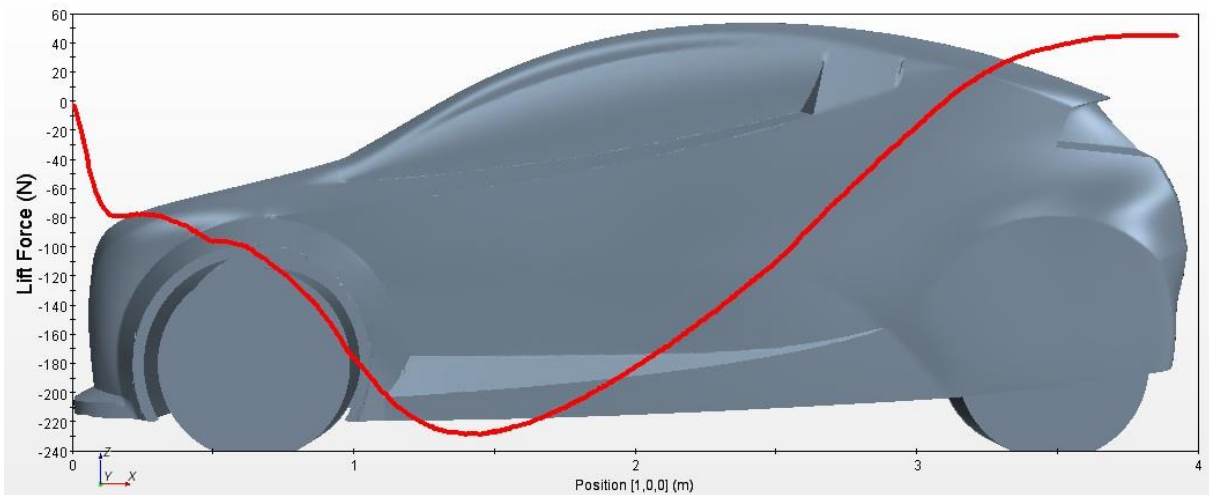
Figure 35- Distance Vehicle - Floor

It is known that the closer the vehicle is off the ground, the lower will be the drag forces. This fact explain the results found on the previous simulations.

Graphs 6 and 7 shows, respectively, Accumulated Drag and Lift Forces:



Graph 6- Accumulated Drag Force



Graph 7- Accumulated Lift Force

As the graph above shows, the accumulated lift force varied from negative values at the front and the middle of the vehicle to positive values at the rear-end. This variation can be explained by the velocity distribution and magnitude along the car, as shown in Figures 36 and 37:

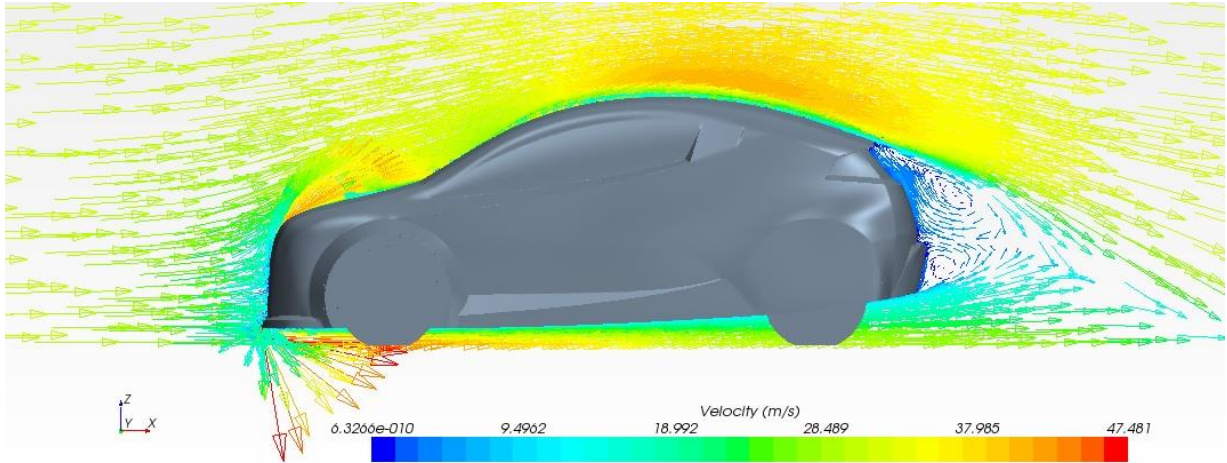


Figure 36- Velocity Distribution Vectors

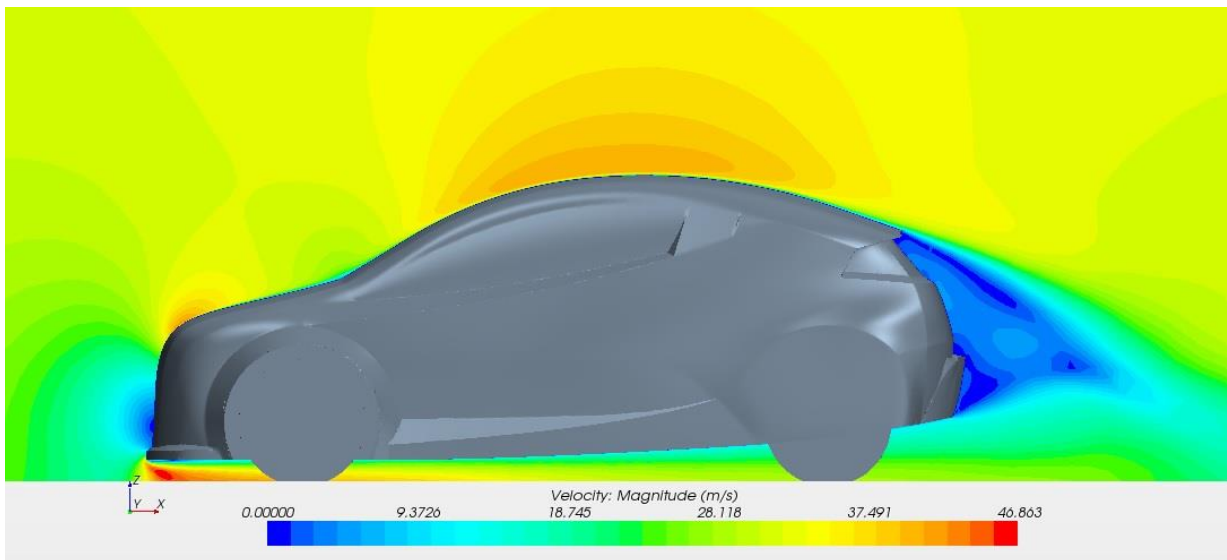


Figure 37- Velocity Magnitude around Vehicle

From the figure above, it is possible to note that at the front, as the flow approaches the vehicle, it enters in a stagnation point, and then accelerates again, around the car.

The acceleration of the flow under the front part of vehicle generates a low pressure region, and consequently, down force (Negative lift force). In fact, it can be noticed on Graph 7.

Figures 38 and 39 illustrates wake formation on the model, while figures 40 and 41 shows the pressure coefficient distribution.

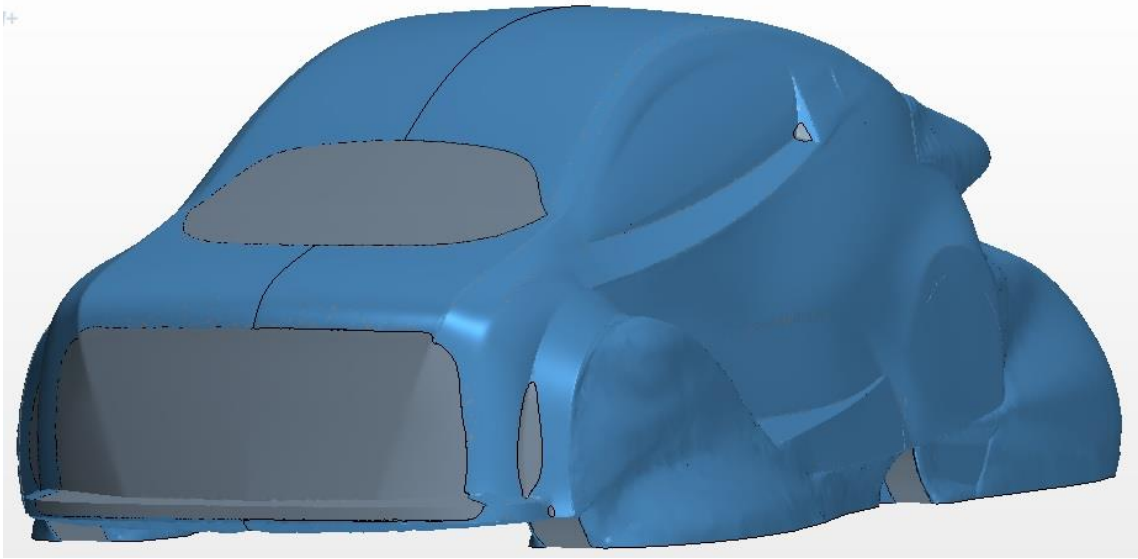


Figure 38- Wake formation (front view)

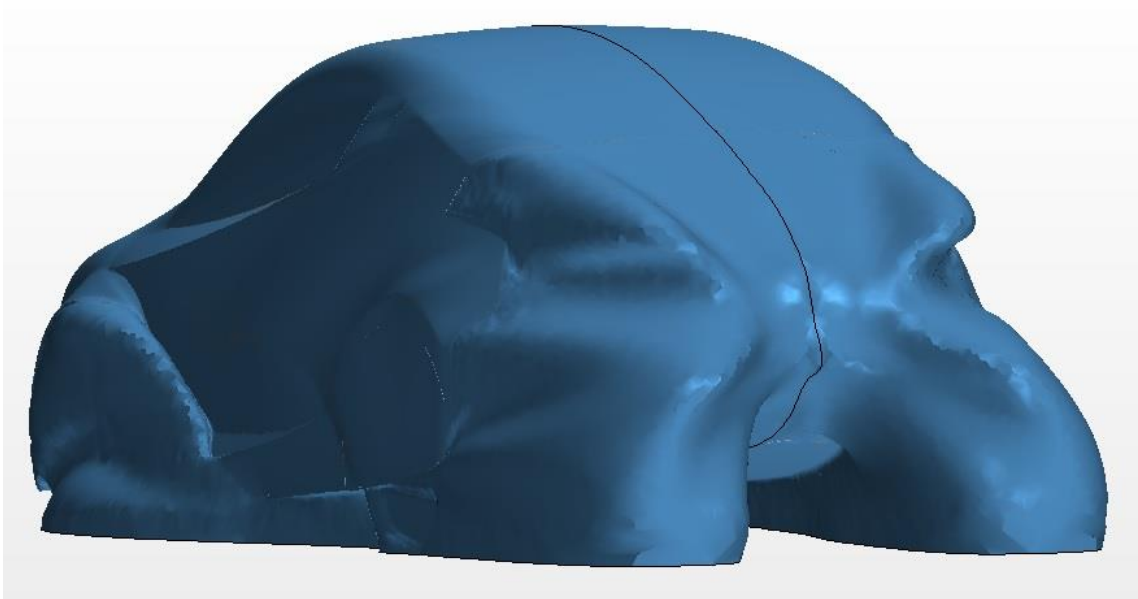


Figure 39- Wake formation (rear view)

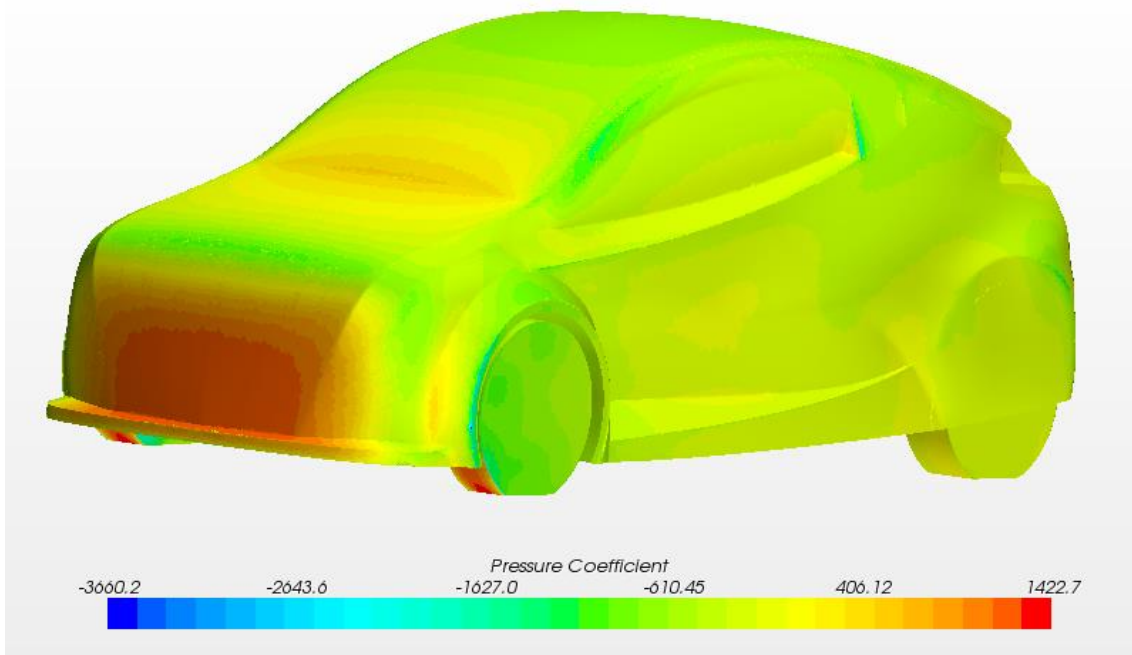


Figure 40- Pressure Coefficient Distribution (Front view)

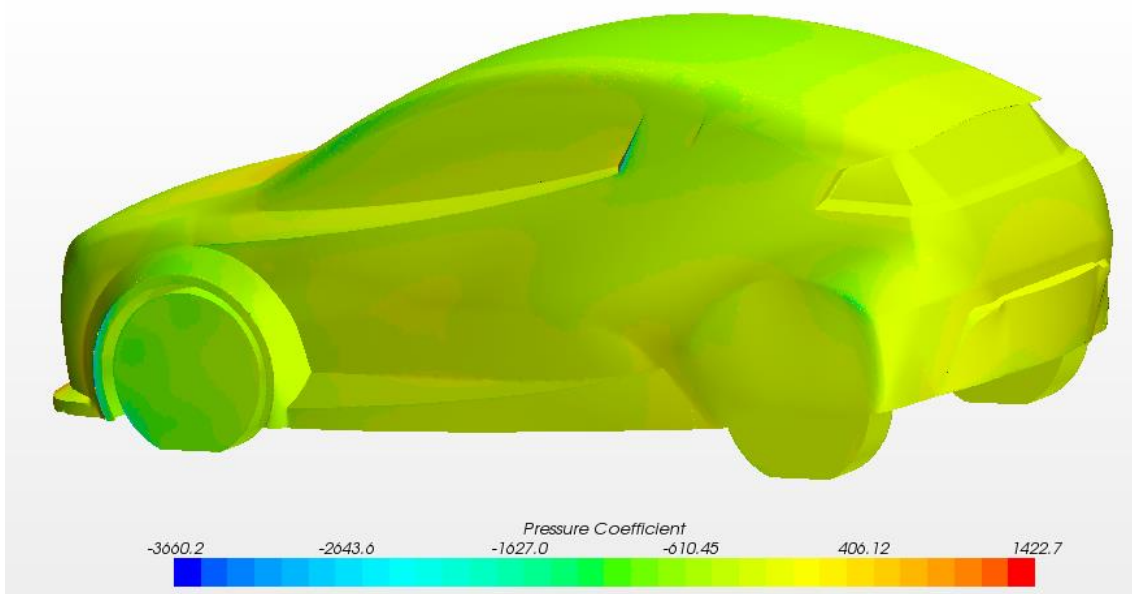
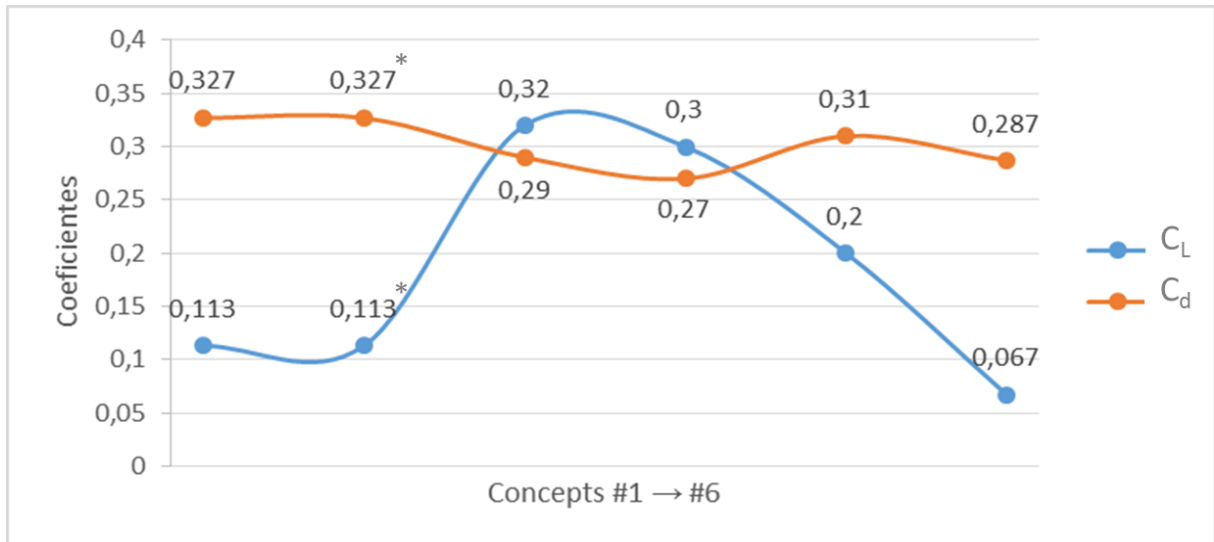


Figure 41- Pressure Coefficient Distribution (Rear view)

Red region indicates high pressure areas, while blue regions indicates low pressure. The front part of the vehicle (red region) concentrates higher pressure areas, therefore, a considerable amount of drag force is generated in this area.

7. CONCLUSION

The Graph below shows the evolution of Drag and Lift coefficients throughout the project.



Graph 8 - Drag and Lift Coefficients Evolution

It is important to notice that coefficients for Concept #2 was not calculated.

As it is possible to check, Concept #4 has the best drag coefficient, but its lift coefficient was considered unsatisfactory.

In short, we can summarize the advantages and disadvantages of Concept #6:

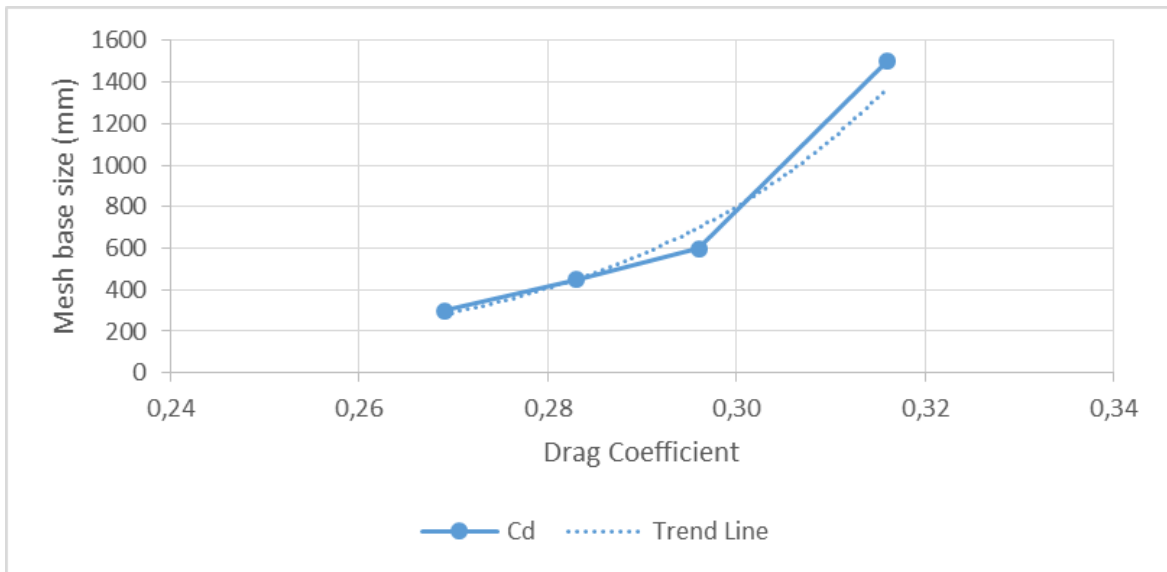
Advantages:

- ❖ Feasible end product;
- ❖ Attractive design;
- ❖ Meets all regulations relating to the safety of pedestrians and passengers;
- ❖ Meets the requirements of ergonomics;
- ❖ A
- ❖ Good results for the lift coefficient;

Disadvantages:

- ❖ Loss of aerodynamic performance (C_d) in comparison with Concept #4;
- ❖ Aim of $C_d \leq 0.25$ was not achieved.

During the CFD simulations, different base sizes of volume meshing were used, and Graph 9 shows the evolution of drag coefficient results according to the base sizes:



Graph 9 - Cd vs Mesh base size

As it is possible to notice, smaller sizes of base size leads to better results of drag coefficient. Unfortunately, it was not possible to run new simulations with base sizes smaller than 300mm because of the computational resource (simulations were taking too much time). As a suggestion for future works, better computational resources or a different license of Star-CCM+ Software would lead to better results.

In order to find better results for drag coefficient, it is important to make certain external modifications. Figures 42 and 43 illustrates regions which can be modified in order to improve aerodynamic performance.

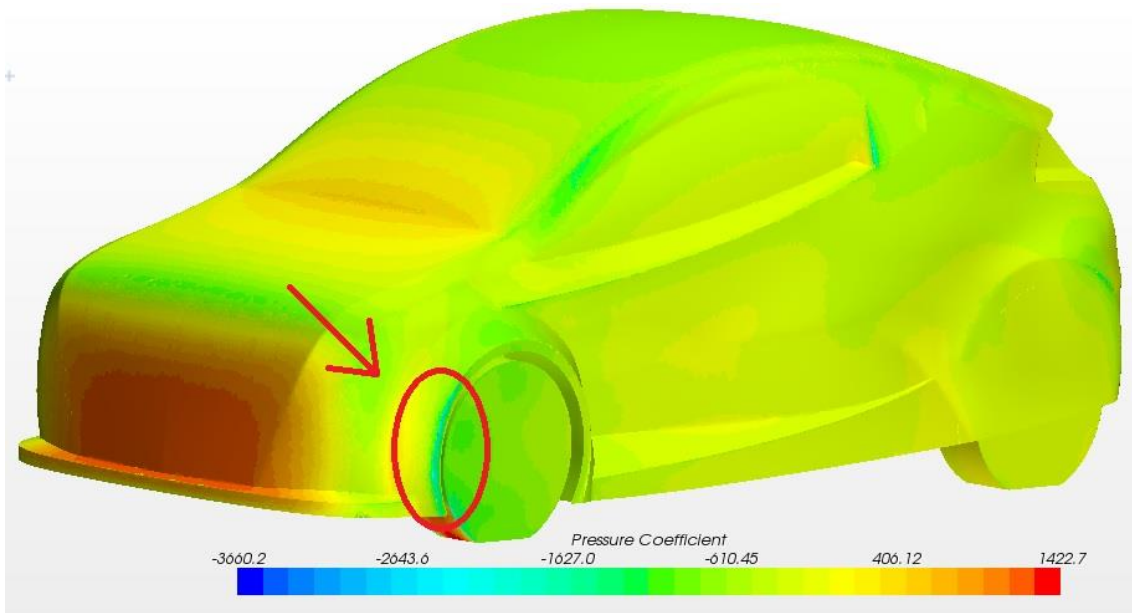


Figure 42- Recommended Modifications

Front wheels arches are low pressure regions, as the figure above shows. In this region, the air flow separates, therefore wake formation occurs.

Regions indicated on figure below are also regions where wake formation occurs and could be modified in order to improve aerodynamic performance.

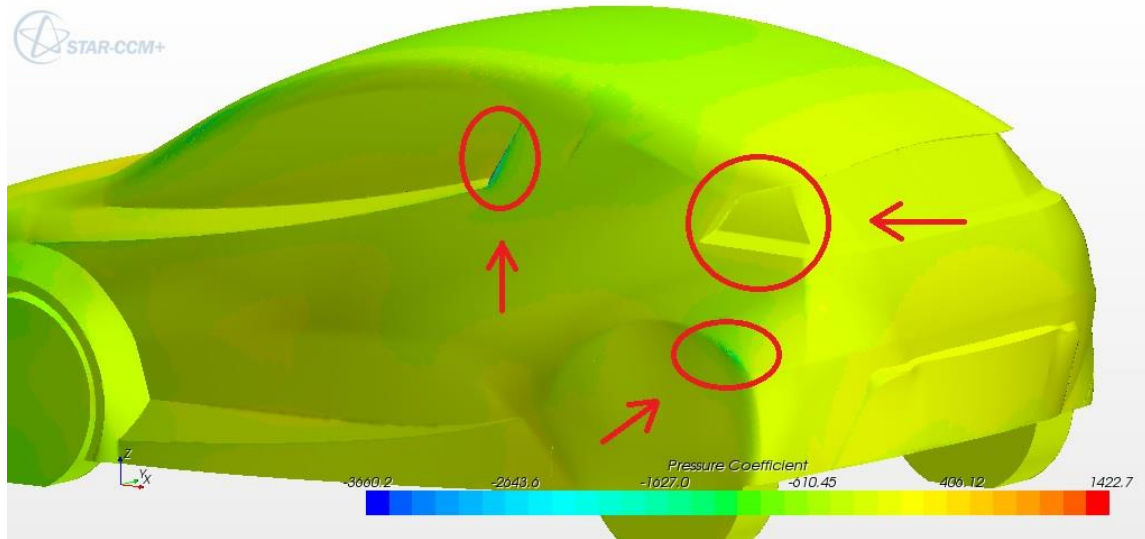


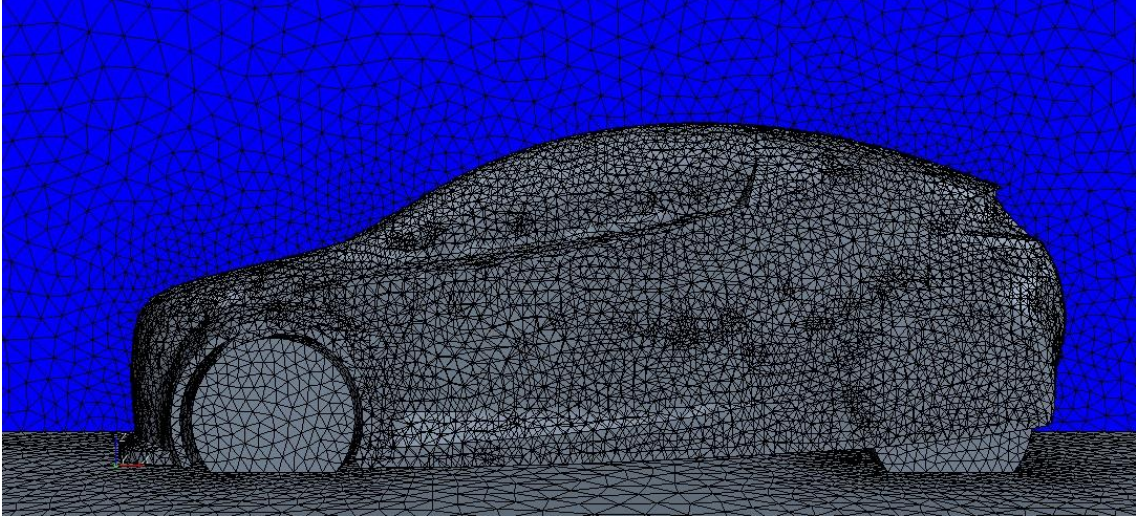
Figure 43- Recommended Modifications

8. REFERENCES

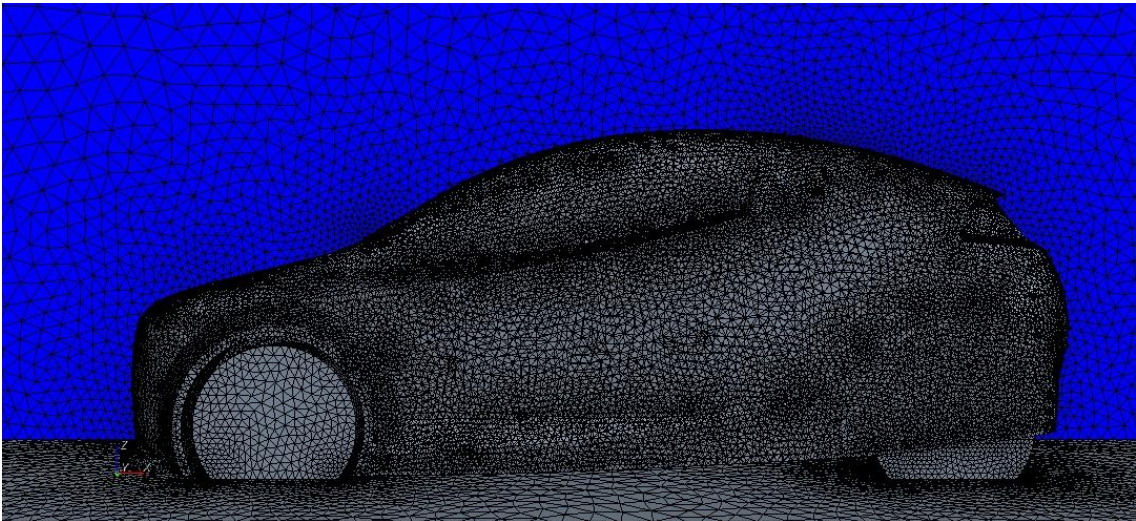
1. Ahmed, S. R. et al (1998) Ed. By Hucho, W. H. *Aerodynamics of Road Vehicles*. 4th ed. Warrendale, USA. Society of Automotive Engineers, Inc.
2. Barnard, R. H. (2009) *Road Vehicle Aerodynamics Design*. 3rd ed. Mech Aero.
3. Businaro, U. L., Dorgham, M. A, International Association for Vehicle Design (1983). *Impact of Aerodynamics on Vehicle Design*. UK: Inderscience Enterprises Ltd.
4. Calnev, D. (2013). *Designing and Manufacturing of a Scale Model for the TARF-LCV Vehicle*. Coventry University.
5. G M Le Good (1998). *A Comparison of On-Road Aerodynamic Drag Measurements with Wind Tunnel Data from Pininfarina and MIRA*. Detroit: SAE International Technical Paper Series.
6. Kasravi, K. (n. d.). *Class Notes: Aerodynamics*. [online] available from <<http://www.kasravi.com/cmu/tec452/Aerodynamics/AeroIndex.htm>> [6th October 2013]
7. Research Councils UK (2013). *Towards Affordable, Closed-Loop Recyclable Future Low Carbon Vehicle – TARF-LCV*. [online] available from <<http://gtr.rcuk.ac.uk/project/D64B3346-249F-49AF-94B4-D90A6F633904>> [28th November 2013]
8. Unlimited Performance Products (2007). *Tips: Aerodynamics*. [online] available from <<http://www.up22.com/Aerodynamics.htm>> [5th October 2013]
9. Vasiu, C. et al, (2013). *TARF-LCV Product Innovation*. Coventry University.

APPENDIX A – Volume Meshes

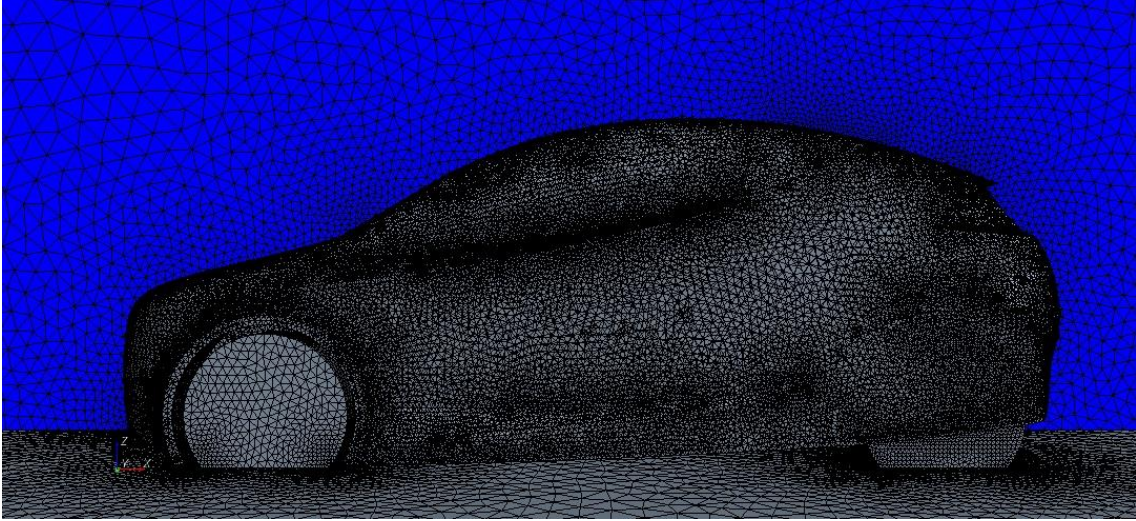
Volume Mesh – Reference Base Size: 1500 mm



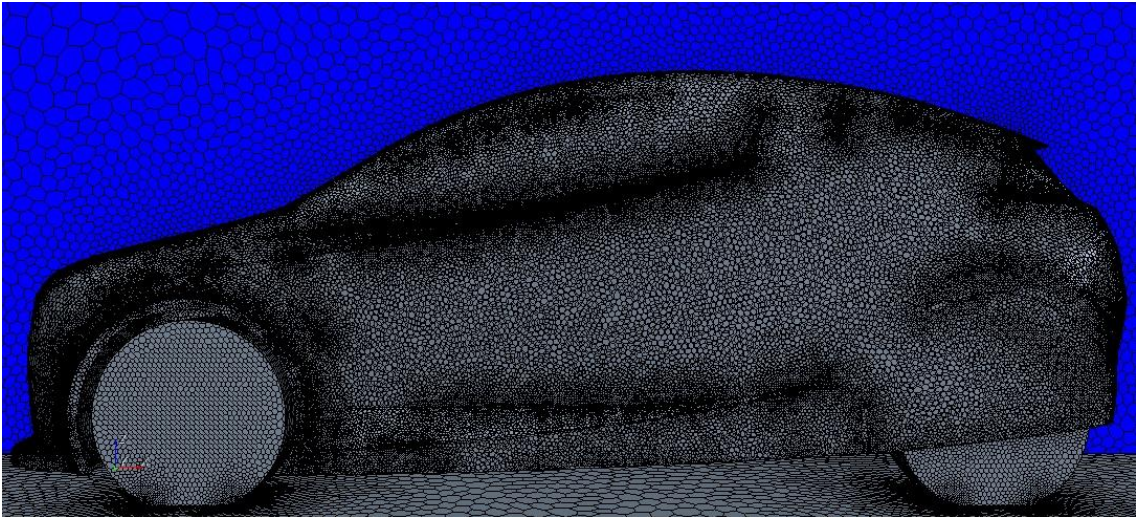
Volume Mesh – Reference Base Size: 600 mm



Volume Mesh – Reference Base Size: 450 mm

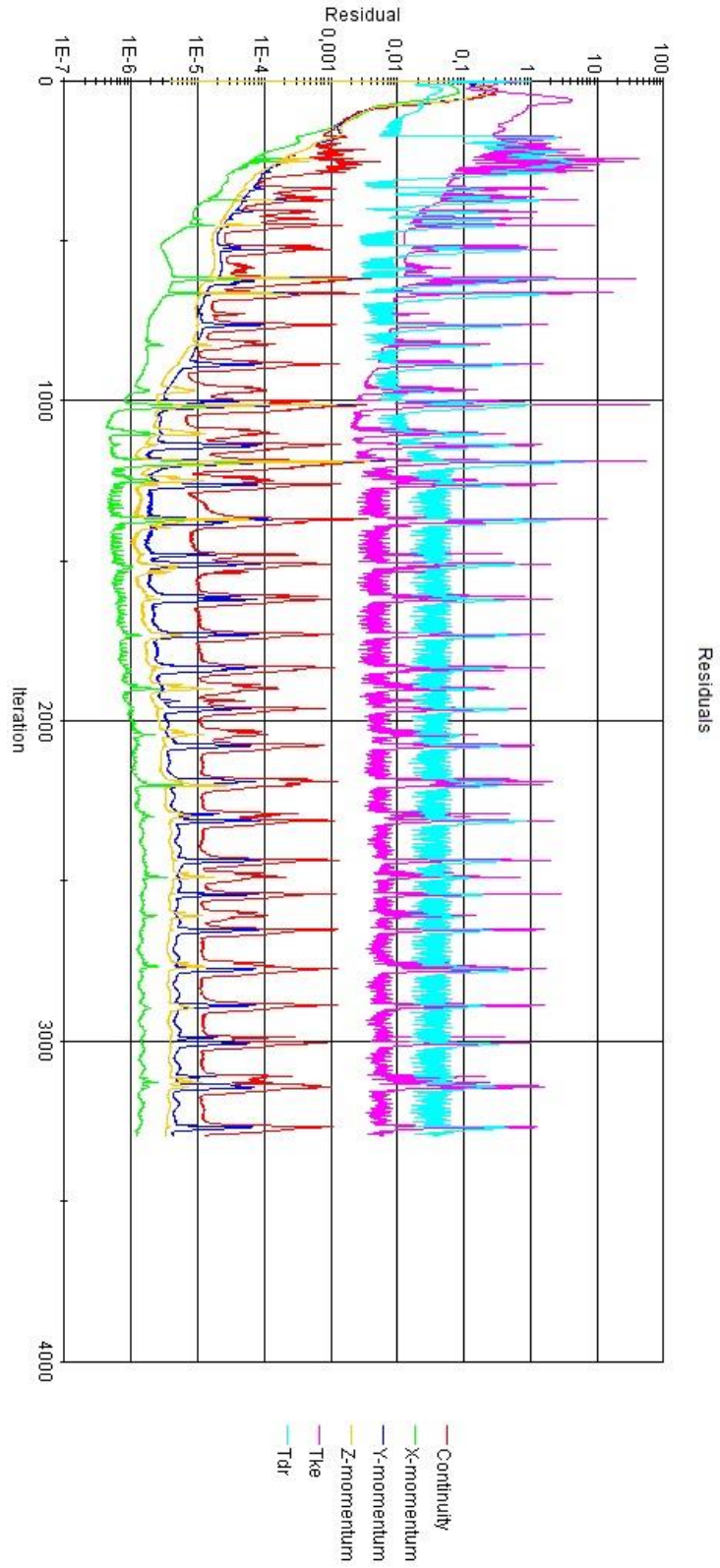


Volume Mesh – Reference Base Size: 300 mm



APPENDIX B – Residuals Plot

450 mm Reference Base Size Simulation



300 mm Reference Base Size Simulation

